Smart Grid Energy Management Staff Exchange

D4.3 Lessons learnt from the existing smart / micro grids. Guidelines for scaling-up the existing infrastructure using mobile connectivity

Revision History

Revision date	Previous revision date	Summary of Changes	Changes marked
22/9/17	-	First issue	

Approvals

This document requires the following approvals:

Name	Partner	Date	Approval (y/n)
Prof. Denia Kolokotsa (Project Coordinator)	TUC	27/9/2016	y
Prof. Margarita Assimakopoulos	UOA	27/9/2016	y
Prof. Diofantos Hadjimitsis	CUT	27/9/2016	y
Prof. Costas Papanicolas	CyI	27/9/2016	y
Prof. Maria Kolokotroni	UBRUN	27/9/2016	y
Dr. Cristina Cristalli	AEA	27/9/2016	y
Fabio Montagnino	IDEA	27/9/2016	y
Dr. Nerijus Kruopis	EGM	27/9/2016	y
Federica Fuligni	EXERGY	27/9/2016	y
Prof. Siew Eang	NUS	27/9/2016	y

Distribution

This document has been distributed to:

Name	Partner	Date
Prof. Denia Kolokotsa (Project Coordinator)	TUC	27/9/2016
Prof. Kostas Kalaitzakis	TUC	27/9/2016
Kostas Gobakis	TUC	27/9/2016

Nikos Kampelis	TUC	27/9/2016
Aggeliki Mavrigiannaki	TUC	27/9/2016
Prof. Mattheos Santamouris	UOA	27/9/2016
Theoni Karlesi	UOA	27/9/2016
Prof. Margarita N. Assimakopoulos	UOA	27/9/2016
Vassilis Lontorfos	UOA	27/9/2016
Ioannis Kousis	UOA	27/9/2016
Prof. Diofantos Hatzimitsis	CUT	27/9/2016
Prof. Costas Papanicolas	CyI	27/9/2016
Alex Lupion Romero	CyI	27/9/2016
Marios Demetriades	CyI	27/9/2016
Marina Kyprianou	CyI	27/9/2016
Andri Pyrgou	CyI	27/9/2016
Prof. Maria Kolokotroni	UBRUN	27/9/2016
Prof. Tatiana Kalganova	UBRUN	27/9/2016
Thiago Santos	UBRUN	27/9/2016
Emmanuel Shittu	UBRUN	27/9/2016
Dr. Cristina Cristalli	AEA	27/9/2016
Riccardo Paci	AEA	27/9/2016
Dr. Laura Standardi	AEA	27/9/2016
Gino Romiti	AEA	27/9/2016
Dr. Daniela Isidori	AEA	27/9/2016
Dr. Nerijus Kruopis	EGM	27/9/2016
Karolis Koreiva	EGM	27/9/2016
Gabija Silienė	EGM	27/9/2016
Fabio Montagnino	IDEA	27/9/2016
Filippo Paredes	IDEA	27/9/2016
Luca Venezia	IDEA	27/9/2016
Pietro Muratore	IDEA	27/9/2016
Federica Fuligni	EXERGY	27/9/2016

Fernando Centeno	EXERGY	27/9/2016
Gozde Unkaya	EXERGY	27/9/2016
Felipe Maya	EXERGY	27/9/2016
Sreenivaasa Pamidi	EXERGY	27/9/2016
Kassim Caratella	EXERGY	27/9/2016
Monica Osorio	EXERGY	27/9/2016
Prof. Siew Eang	NUS	27/9/2016

645677 — SMART GEMS — H2020-MSCA-RISE-2014
D4.3 Lessons learnt from the existing smart / micro grids. Guidelines for scaling-up the existing
infrastructure using mobile connectivity

Table of Contents

645677 — SMART GEMS — H2020-MSCA-RISE-2014
D4.3 Lessons learnt from the existing smart / micro grids. Guidelines for scaling-up the existing
infrastructure using mobile connectivity

List of Figures

List of Tables

Summary

In this report various research and development activities related to the analysis and monitoring of smart microgrids are presented. Performance evaluation and control of smart microgrids at AEA, Loccioni and Technical University of Crete campus have been thoroughly explored. Algorithms for energy and asset management, successful exploitation of smart meters in smart grids, data mining techniques and energy predictions are exploited to shape new advanced modelling and control methodologies for future district and community applications.

In this context, researchers from industry and academia have worked together to build and exchange knowledge in various fields as indicated in Table 0-1:

Table 0-1: Seconded researchers and activities presented in Deliverable 4.3

Researchers	Sending Organisation	Organisation of Destination	Research Field
Konstantinos Gobakis (author)	Technical University of Crete	Elgama - Elektronika	Smart meter communication security and testing
Nikos Kampelis (author)	Technical University of Crete	Elgama - Elektronika	Mathematical model and design of flicker meter for application in smart meters
Aggeliki Mavrigiannaki (author)	Technical University of Crete	AEA, Loccioni	Prediction of excess power production of the Leaf micro-grid
Emmanuel Shittu (author)	UBRUN	Elgama - Elektronika	Mathematical model and design of flicker meter for application in smart meters
Konstantinos Stokos	Cyl	Elgama - Elektronika	Smart meter communication security and testing
Elli Tsirintoulaki (/ Nikos Kampelis) co-authors	Technical University of Crete	EXE	Data analysis of smart metering, load predictions and sizing of PV system in TUC microgrid
Lukas Samulevicious (work in progress)	Elgama - Elektronika	Technical University of Crete	Smart static electricity meters PLC testing in TUC microgrid

645677 — SMART GEMS — H2020-MSCA-RISE-2014
D4.3 Lessons learnt from the existing smart / micro grids. Guidelines for scaling-up the existing
infrastructure using mobile connectivity

1. Introduction

Limitations in the functionality of the current power grid along with the increasing penetration of renewables, advanced metering infrastructure investments and the gradual 'opening' of markets to accommodate more players and new business models are all factors contributing to advancements in the field of Distributed Energy Resources (DER) management.

This is a highly demanding and complicated process since it requires the continuous collection and systematic hierarchical analysis of multiple data related to the operating energy production, consumption and storage systems, facilities structural information, indoor conditions, human behavior, microclimate and weather conditions.

State of the art techniques and scientific research link future district energy management applications with real time dynamic processing of data measured by a wide network of meters and sensors connected in the Internet of Things.

Various techniques and tools can be potentially utilized to assist and facilitate this process including smart metering data analysis and processing, distributed energy resources management techniques, power forecasting, demand response and users engagement.

Smart metering is crucial to transfer dynamically exploitable data in a reliable and effective way. Smart meters and advanced metering infrastructure can play an important role in managing the grid based on nodal data regarding consumption and / or production providing useful information for the identification of opportunities, vulnerabilities and solutions.

Smart energy data is particularly important in specific when dealing with the high intermittency of renewable energy generation, volatility of loads and ultimately with balancing supply and demand. In this framework power quality in the grid is a crucial aspect related to reliability and robustness. Significant power disruptions, the malfunctioning or damage of connected equipment are linked to consumers' perception for low quality of service. Most importantly, voltage fluctuations i.e. flickering can pose potential health risks depending on the occasion, severity and duration. Analysis and evaluation of power quality is therefore vital for the identification of problem sources and targeted

645677 — SMART GEMS — H2020-MSCA-RISE-2014
D4.3 Lessons learnt from the existing smart / micro grids. Guidelines for scaling-up the existing
infrastructure using mobile connectivity

intervention. Consideration of distributed voltage flickering measurements provides a solid basis for spatial and time domain resolution.

On the other hand the management of interconnected renewable resources, storage and loads as in the case of microgrids is receiving increasing attention from both industry and academia. This field is an open space for research and innovation linking different renewable generation technologies with different varying loads in real time. This is a challenging task involving design and optimisation considerations and robust controls, determined by the specificities of each case.

645677 — SMART GEMS — H2020-MSCA-RISE-2014
D4.3 Lessons learnt from the existing smart / micro grids. Guidelines for scaling-up the existing
infrastructure using mobile connectivity

2. Methodology

The methodology of the activities presented resides in the framework of the Smart GEMS project (Figure 2-1). Following research activities in the framework of Work Package 3 dealing with integrated design, operational efficiency, components, services and controls at building level, activities are now focusing on district level. Work package 4 is related to the optimised operation of renewables (D4.1), cost benefit analysis of polygeneration for smart communities (D4.2) and lessons / guidelines for scaling up existing smart / micro grid infrastructure using mobile connectivity (D4.3).
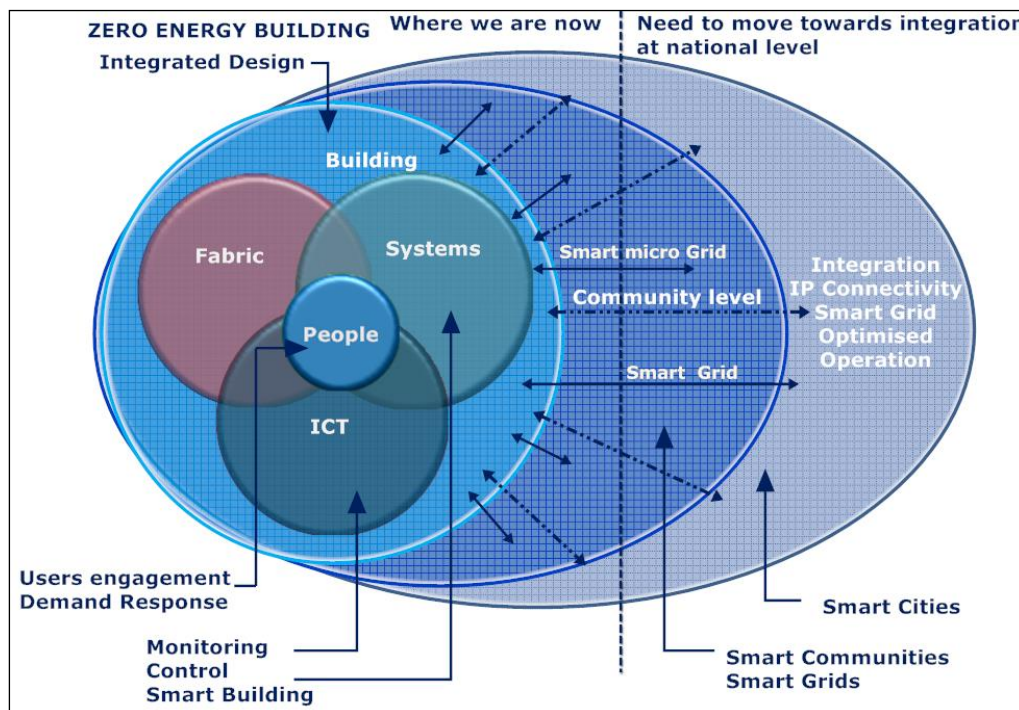
Figure 2-1: The methodological approach of smart technologies

In this context, research activities focused largely on the two smart / micro grids of the project. TUC campus distributed power measurements were used to perform data interpretation, predictions using Artificial Neural Network models and sizing of PV installations. Leaf community distributed power measurements were exploited to predict excess power and develop a strategy for the charging of thermal storage. Testing of predictions demonstrated the feasibility of this approach and future actions have been drawn to determine how it can be utilized in practical applications in the steps to follow.

645677 — SMART GEMS — H2020-MSCA-RISE-2014
D4.3 Lessons learnt from the existing smart / micro grids. Guidelines for scaling-up the existing
infrastructure using mobile connectivity

On the other hand staff exchange has been fruitful in the design and development of smart metering applications for voltage flickering and data security functions. Progress in this direction has been productive but also enlightening of the technical challenges faced by industrial partners and how academic partners be actively involved.

In all the aforementioned cases links between the academic and industrial organisations have been strengthened and efforts are headed towards extended collaborations in the near future.

645677 — SMART GEMS — H2020-MSCA-RISE-2014
D4.3 Lessons learnt from the existing smart / micro grids. Guidelines for scaling-up the existing
infrastructure using mobile connectivity

3. Research projects and activities in existing smart / micro grids

3.1 Prediction of excess power production of the Leaf micro-grid

The requirement for clean energy, energy efficiency and cost-efficient energy management has given rise to the investigation of transition from traditional energy distribution grids to smart micro-grids. In traditional electricity grids energy is produced centrally and distributed to the various energy consumers that are connected to the grid. Traditional grids lack flexibility in power generation and load operation [1]. A micro-grid comprises distributed energy sources, energy loads and storage components, thus forming a semi-autonomous entity with energy management capabilities. Moreover, a micro-grid can operate connected to the main grid or in island mode [2]. For the purpose of reliable and efficient operation the Energy Management System (EMS) has become an essential component of micro-grids [2] [3].

EMS assists in the optimization of power distribution within a micro-grid through the application of appropriate controls. Measuring and monitoring and control equipment connected through Information and Communication Technologies (ICT) are necessary for "building" an EMS. These assets combined with advanced energy management techniques make a micro-grid smart [1], [4], [5], [6]. A smart micro-grid communicates with its components and through the EMS controls its loads so as to achieve an efficient and cost-effective operation. In [7] an energy management algorithm is tested for optimum integration and operation of a PV array and a battery for serving a micro-grid's loads. In [8] two algorithms are proposed and tested on an existing micro-grid, one for energy scheduling and one for demand response. Increased efficiency and occupant satisfaction has been achieved by the EMS applied in a University Campus [5]. Load forecasting is invaluable to micro-grid energy management [5], [6], [8], [9]. Load forecasting for controlling charge and discharge of an electrical storage has been studied in [10] as well as in [11]. Depending on the forecasted period three types of forecasting are recognised [6], [9]:

645677 — SMART GEMS — H2020-MSCA-RISE-2014
D4.3 Lessons learnt from the existing smart / micro grids. Guidelines for scaling-up the existing
infrastructure using mobile connectivity

- Short-term forecasting: 1h to 1week for optimum
- Medium-term forecasting: 1week to 1year
- Long-term forecasting: 1year to decades ahead

Two methods for load forecasting have been recognised in literature, statistic mathematical models and artificial intelligence models [6], [9]. Artificial Neural Networks (ANN) are artificial intelligence models widely used for forecasting providing high accuracy [6], [9]. ANN have been extensively used for short-term load prediction [9], [11]. In [12] a multi-layer perceptron neural network that uses load and weather data was applied in order to forecast the daily load of a suburban area. In [13] a feed forward artificial neural network for hourly demand prediction is tested and the proposed algorithm is able to achieve a high prediction accuracy.

The present report presents the 24h load forecasting of Leaf micro-grid using artificial neural networks. The purpose is to predict the day ahead excess production of the micro-grid so as to apply appropriate controls for its utilisation.

3.1.1 The Leaf micro-grid

The Leaf micro-grid is the micro-grid of the Leaf Community, in Angeli di Rosora, Italy (Figure 3-1).

Figure 3-1 The Leaf Community microgrid

645677 — SMART GEMS — H2020-MSCA-RISE-2014
D4.3 Lessons learnt from the existing smart / micro grids. Guidelines for scaling-up the existing
infrastructure using mobile connectivity

The energy production sources connected to the grid are:

- a micro-hydropower plant, of 48kWp
- four rooftop PV installations of total 421.3kWp
- a dual axis Solar Tracker of 18kWp

Five buildings are currently connected to the micro-grid:

- The Leaf Lab, industrial building
- The AEA, office building
- The SUMMA, office building
- The Leaf Farm, office building
- The KITE, industrial building

All buildings are equipped with ground water heat pumps (GWHP). A 224kWh electrical storage system and a thermal storage with heat capacity 523.25kWh/K are also part of the micro-grid.

All the previously mentioned power loads, renewables and storage components are connected in parallel to one single Point of Delivery (POD). All nodes as well as the collective operation of the micro-grid are monitored and controlled via My Leaf web based platform.

The rooftop PVs are installed on four of the five interconnected buildings of the micro-grid. The production by each rooftop PV installation is consumed by the respective building first. If there is residual production, it is fed to the micro-grid. The production of the micro-hydropower plant is also fed to the micro-grid. When the production is not enough to cover the micro-grid's loads, energy is withdrawn from the main grid. Energy is also given to the main utility grid if the demand of the micro-grid has been fulfilled, storages are fully charged and there is excess production. Regarding the storages, both have been recently connected to the grid and their operation and integration currently being tested. In the present work the integration of the thermal storage with the micro-grid is studied. Specifically, the availability of excess production in the micro-grid during weekends is of interest, so as to schedule the charging of the thermal storage using this excess production.

The thermal storage is connected to the Leaf Lab and the automation system for its charge and discharge has been set considering this building. Currently, the automation system is set to charge the thermal storage during weekends, when there is excess production from Leaf Lab's PV. This kind of automation will charge the storage when energy is not needed form Leaf Lab, but it could be needed from the micro grid. Consequently, there is a requirement to change the settings so that the thermal storage will be charged when there is real excess production at micro-grid level. To this end, excess production of the micro-grid during weekends needs to be predicted in a robust way so that charging of the thermal storage is controlled accordingly.

3.1.2 System description

Ground water heat pumps

There are three water to water heat pumps in Leaf Lab. GWHP1 is connected to the chilled beams installed in the offices for space heating and cooling. GWHP2 and GWHP3 are connected to four HVAC units that service the offices, the laboratory and the warehouse.

The heat pumps are connected to the storage as shown in Figure 3-2. GWHP2 and GWHP3 are used for charging the thermal storage. When the thermal storage is discharged, thermal energy is provided to the chilled beams, thus avoiding activation of GWHP1 during the first three days of the week.

Thermal storage

The TES is a water tank with dimensions 12.3 X 11 X 3.4 m (400m³).The water tank is buried and insulated with16 cm of XPS. The heat stored is sensible heat intended to cover the thermal loads of Leaf Lab. The thermal storage is charged during weekends using the excess production of the Leaf Labs' rooftop PV installation. The excess production is used to operate GWHP2 and GWHP3.

645677 — SMART GEMS — H2020-MSCA-RISE-2014
D4.3 Lessons learnt from the existing smart / micro grids. Guidelines for scaling-up the existing
infrastructure using mobile connectivity
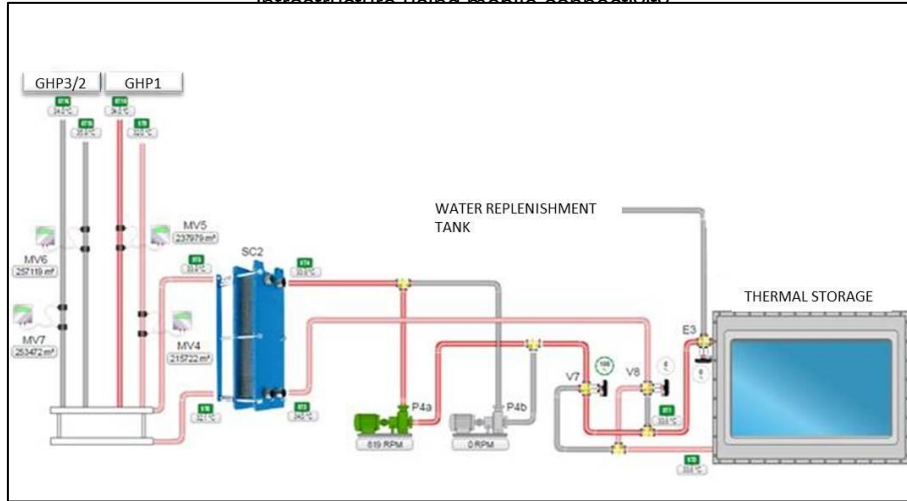
Figure 3-2: Thermal storage - GWHP connection schema

System settings

The charging process begins when there is an excess in Leaf Lab's PV power production over 60kW. This is the threshold for activation of GWHP3. After activation of GWHP3, if there is excess of 50kW, GWHP2 is activated.

The activation of the heat pumps for charging the thermal storage is allowed only during weekends, from 8:00am to 16:00pm in winter weekends and from 7:00am to 18:00pm in summer weekends. The pumps are switched off at the end of each schedule or if PV production is significantly reduced over a sustained period of time. In case PV power is instantly reduced power is withdrawn from the grid in order to keep the heat pumps, which provide heat to the thermal storage, activated. For the deactivation of the heat pumps if the power from the grid is greater than 130kW GWHP3 is switched off and following this GWHP2 is switched off when energy withdrawn from the utility grid exceeds 90kW.

3.1.3 Power production data

Power data as well as environmental data have been collected from the My Leaf platform. The power production of each energy source and the power taken from and exported to the main grid are being measured.

The total production of the micro-grid can be calculated as follows:

$$P_{MG} = P_{LLPV} + P_{AEAPV} + P_{SUMMAPV} + P_{KITEPV} + P_{TUV} + P_{HYDRO4} \quad (1)$$

Where:

645677 — SMART GEMS — H2020-MSCA-RISE-2014
D4.3 Lessons learnt from the existing smart / micro grids. Guidelines for scaling-up the existing
infrastructure using mobile connectivity

P_{LLPV} is the power production of the Leaf Lab PV, in kW

P_{AEAPV} is the power production of the AEA PV, in kW

$P_{SUMMAPV}$ is the power production of the SUMMA PV, in kW

P_{KITEPV} is the power production of the KITE PV, in kW

P_{TUV} is the power production of the solar tracker, in kW

P_{HYDRO4} is the power production of the micro-hydro power plant, in kW

The production of the micro-grid is self-consumed and excess production is given to the main grid. Since there are measured data of the power exported to the grid, the power production self-consumed at any time in the micro-grid can be calculated as follows:

$$P_{SC} = P_{MG} - P_{OUT} \quad (2)$$

Where:

P_{SC} is the power production self-consumed, in kW

P_{OUT} is the amount of excess power production that is exported to the main-grid, in kW

3.1.4 Data analysis

In Figure 3-3 and Figure 3-4 it can be observed that there is a positive correlation between excess production and irradiance values, especially during peaks.

645677 — SMART GEMS — H2020-MSCA-RISE-2014
D4.3 Lessons learnt from the existing smart / micro grids. Guidelines for scaling-up the existing
infrastructure using mobile connectivity
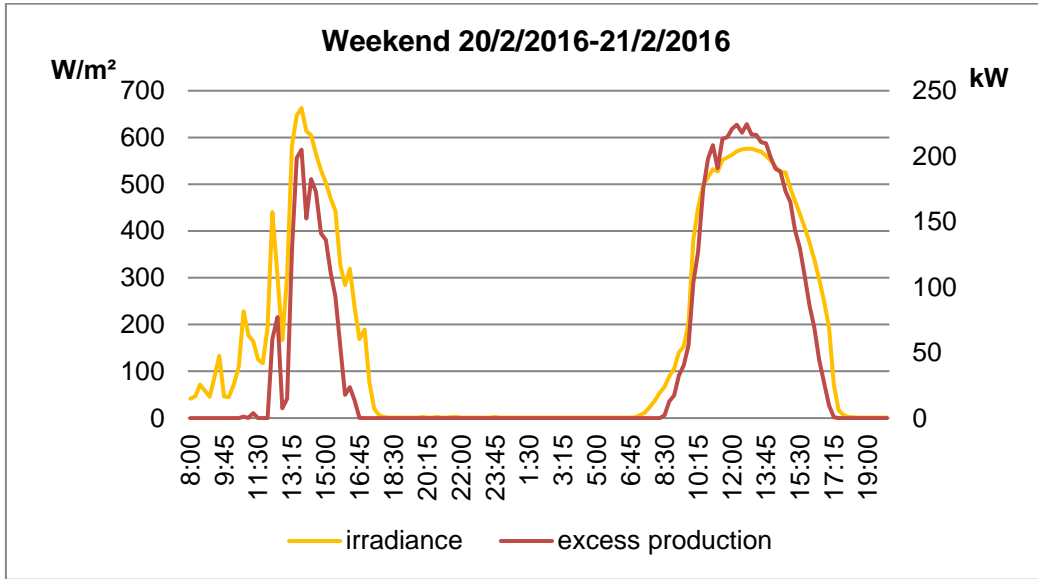
Figure 3-3: Excess production plotted along irradiance for the weekend 20/2/1026-21/2/2016
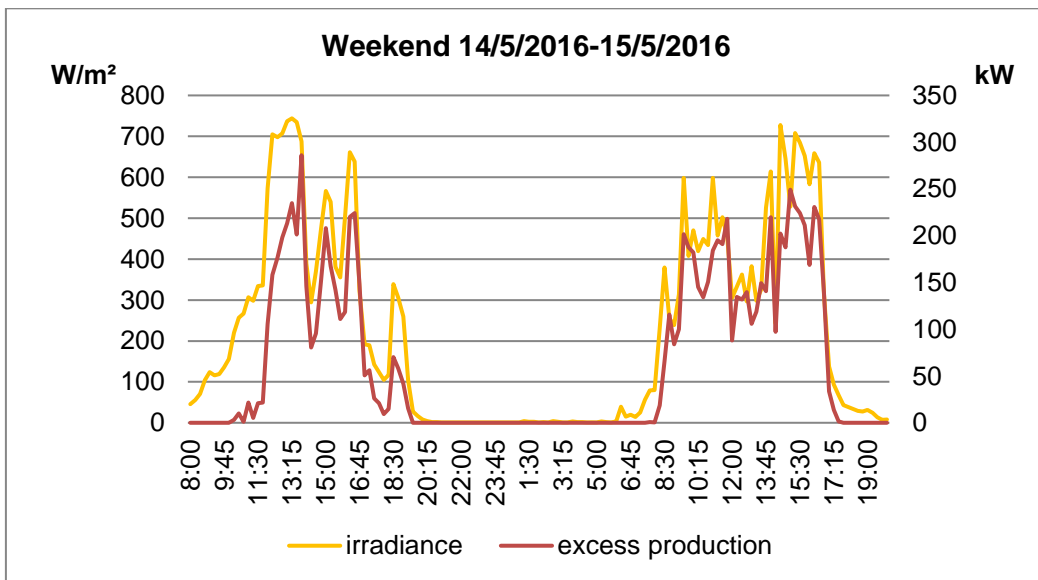
Figure 3-4: Excess production plotted along irradiance for the weekend 14/5/2017-15/5/2017

It can also be observed from Figure 5 that excess production follows the trend of total production.

645677 — SMART GEMS — H2020-MSCA-RISE-2014
D4.3 Lessons learnt from the existing smart / micro grids. Guidelines for scaling-up the existing
infrastructure using mobile connectivity
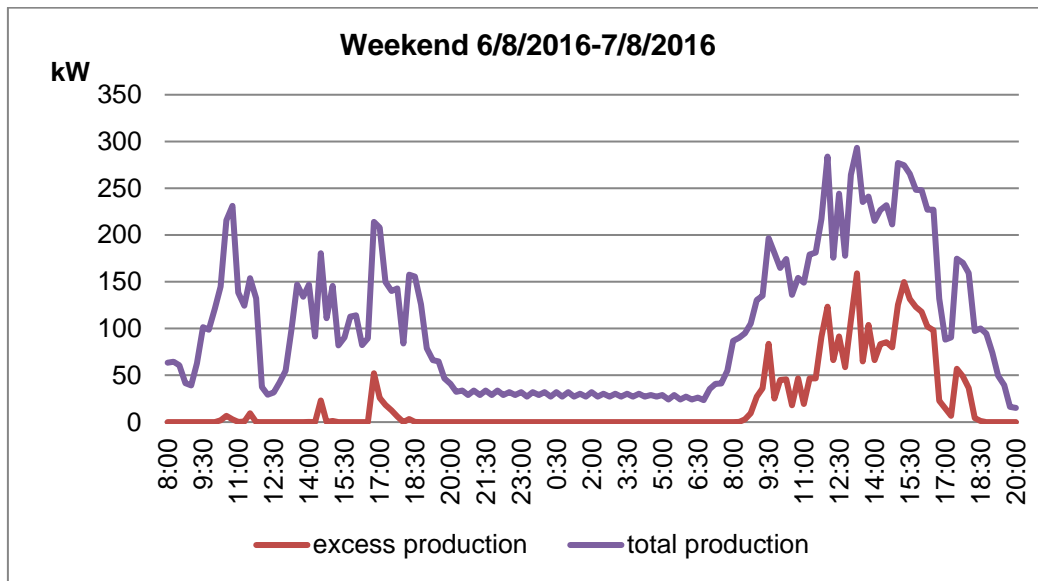
Figure 3-5: Excess production plotted along total production

3.1.5 Predictions using Artificial Neural Network (ANN)

The collected data is used for prediction of excess power of the micro-grid. A good prediction of excess production has to be achieved. For this purpose the Matlab [14] Neural Network (NN) tool was utilised. Alternative combinations of input parameters were tested so as to investigate which set of input parameters were suitable for achieving an accurate prediction of excess production. Furthermore alternative training algorithms were tested and neural network structures in order to conclude which algorithm and structure could give the best prediction results.

3.1.6 NN model setup

The excess production of energy that can be used for charging the thermal storage can be determined from the measured data of power exported to the main grid. The prediction of excess production is a non-linear autoregressive problem. Past values of excess production as well as past values of day, time, irradiance, temperature and total production were used for prediction of excess power in 24h time horizon.

From equations (1) and (2) it can be deduced that excess production is related to parameters that determine production. For prediction of PV production, day of the week, time of day, temperature and radiation have been used as inputs

[10], [15]. Prediction of hydro power production using as inputs the river water level and machine water level was attempted in [10] but a high accuracy prediction could not be achieved.

As a first step, day of the week, time of day and irradiance was used for prediction of excess production. Subsequently, a second prediction approach is tested using the first step's inputs plus ambient air temperature as input. A third prediction model is attempted using as input parameters the day of the week, the time of the day and total micro-grid production since, as observed in Table 1, excess production follows the trend of total production.

Table 1: Input data for each prediction

	Inputs	Target	Output
1st prediction	day of week time of day irradiance	excess production (P_{OUT})	excess production (P_{OUT})
2nd prediction	day of week time of day irradiance temperature	excess production (P_{OUT})	excess production (P_{OUT})
3rd prediction	day of week time of day micro-grid production	excess production (P_{OUT})	excess production (P_{OUT})

3.2 Data analysis of smart metering, load prediction and sizing of PV systems in TUC microgrid

District level energy planning and design must focus on a central goal or vision. This vision is realistically shaped by numerous factors such as the current status of the economy, the market, technological progress and available resources. Equally importantly the vision for energy planning needs to be ambitious and effective while counterbalancing human activity associated environmental impact, risks and challenges as identified by climate change at local and global scale.

District level energy planning must be sustainable from an environmental and a financial perspective considering short, medium and long term steps. This involves in some cases complexities related to the conflicting priorities of stakeholders i.e. property owners, the level of engagement towards setting and reaching a specific goal, different opinions etc.

Policy measures, regulatory reforms and finance instruments at EU level have targeted energy savings in the building sector, renewable energy generation and storage, smart grid deployment and advanced metering infrastructure developments, market liberalization, demand response etc. Despite the commitment to the achievement of specific goals linked to energy efficiency and CO_2 equivalent emissions reduction at EU level, efforts need to be shared and owned by the majority of the developed and developing world for a reverse direction to take effect.

At local level, the transformation of buildings and districts in zero, near zero or positive energy facilities is the vision which can lead the essential changes at global level.

In the case of a university campus, numerous buildings, facilities and users co-exist and make use of a subsystem of the main electrical power grid which can under certain conditions operate in autonomous or semi-independent mode.

To achieve this a sustainable plan needs to be developed and implemented to encapsulate the following fundamental principles in a proactive, creative and innovative way: a) Minimization of energy consumption by increasing the

645677 — SMART GEMS — H2020-MSCA-RISE-2014
D4.3 Lessons learnt from the existing smart / micro grids. Guidelines for scaling-up the existing
infrastructure using mobile connectivity

operational energy efficiency of facilities, b) maximization of energy production from renewables, c) effective integration of state of the art energy management techniques and technologies.

The scope of this report is directly related to the development and integration of energy management techniques in a microgrid but also linked to the maximum utilization of energy production from renewables.

In this respect the approach presented hereafter partly concerns the utilisation of data to establish robust, cost effective, environmentally sustainable energy management at district level. The proposed approach can be utilized at districts or communities of different operational context such as those hosting industrial or commercial activities.

Work presented in this report deals with nodal data analysis of campus wide electrical energy consumption distributed measurements and neural network models power predictions. Power load and demand predictions can be exploited in advanced energy management applications when the utility grid is at stress or the cost of energy production is high as well as for the identification of energy and cost savings due to the implementation of demand response strategies.

3.2.1 Analysis of the existing microgrid in TUC Campus

The analysis of the existing status with regards to the facilities and the energy conversion systems has been made by exploiting data from various sources such as electromechanical installations designs, data from the installed energy meters in the Campus and information provided by the technical department of TUC [16].

Figure 3-6: **TUC Campus and facilities**

 presents the different facilities of TUC as captured by Google Earth. Figure 3-7 indicates the electric energy meters located in the campus of Technical University of Crete. Table 3-1 outlines the main energy transformation systems in the various departments.

645677 — SMART GEMS — H2020-MSCA-RISE-2014
D4.3 Lessons learnt from the existing smart / micro grids. Guidelines for scaling-up the existing
infrastructure using mobile connectivity

A2 – Amphitheatre	K1 \
B2 – Restaurant	K2 – ENVENG
D1 – Library (new building)	K3 /
D2 – Technical Service	K4 – ARCH
D3 \	L – ECE/Sciences
D4 – PEM	M1 \
D5 /	M2 \
E1 – Library (old building)	M3 – MRED buildings
Z – Sports facilities	M4 /
H – Dormitories	M5 /

PEM buildings
Sports Facilities
Dormitories
ENVENG buildings
ECE/Building of Sciences
MRED buildings

- PEM – Production Engineering & Management
- ENVENG – Environmental Engineering
- ECE – Electrical and Computer Engineering

645677 — SMART GEMS — H2020-MSCA-RISE-2014
D4.3 Lessons learnt from the existing smart / micro grids. Guidelines for scaling-up the existing
infrastructure using mobile connectivity

	• MRED – Mineral Resources Engineering Department • ARCH – Architectural Engineering

Figure 3-6: TUC Campus and facilities
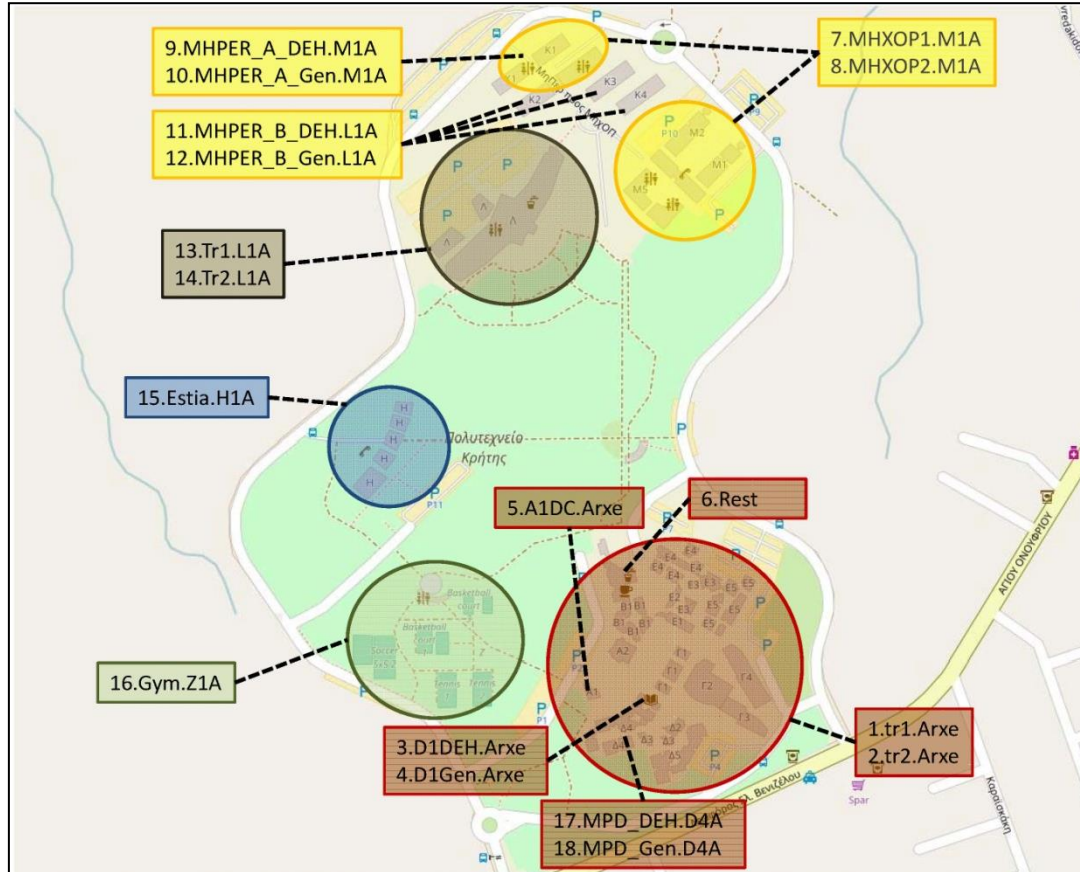
Figure 3-7: Smart Meters map

Table 3-1: Installed systems in the Campus of TUC

	Air Handling Unit System (AHU) Variable Refrigerate Volume Inverter with independent heating/cooling units multi-split type
Environmental Engineering Department	• K1: 3x20hp (14.71kW) in zones 1,2,3 and 1x10hp (7,35kW) in zone 4 • K2 (old section): 9x15 hp (11.03kW) in the zones 1-11, 2x3kW in the zones UPS • K2 (new section): 150kW • Ventilation: fresh air at 5.20m³/h for the K1 and 3.850m³/h for the K2 (old section) • K3: 240kW (6 systems 40kW heating-cooling) • K4: 240kW (6 systems 40kW heating-cooling)

	• DHW (Domestic Hot Water): 11 solar collectors x 1.8m², storage tank DHW 800l (and boiler 600l) with electrical resistances 2x8kW • Lighting Units: 4x18W, 2x36W, 2x18W, 1x18W, 1x8W • Back-up diesel generator and UPS for lighting and safety loads • Low power rooftop and ground PV units
Building of Sciences / Electrical and Computer Engineering	• HVAC:13 AHU 950kW, 32 external units (VRV), 31x100.000 BTU/h and 1x30.000 BTU/h (COP heating=2.86, COPcooling=2.66) • 49x24.000 BTU/h, 103x18.000 BTU/h, 25x12.000 BTU/h, 37x9.000 BTU/h • Lighting: 174 kW • Building Energy Management System • Back up diesel generator and UPS for lighting and safety loads
PEM (Production Engineering Management)- University Facilities	• HVAC:55kW A2 (amphitheater), 30 kW (Old Library), 118.4kW (New Library), ~600 split units of 1.5kW • Diesel boilers 450.000kcal/h, 700.000kcal/h and 50.000kcal/h • Lighting: 4.63kWh/m² (D5) • UPS • Data centre
MRED (Mineral Resources Engineering)	• HVAC 800kW • Air-cooled water heat pump for heating and cooling needs of Mineral Resources Engineering (MRED) buildings, of 290 kW heating and cooling capacity. • DHW: Solar collectors in M2 and M3 with boiler • Lighting: • Back up diesel generator and UPS for lighting and safety loads
Dormitories	• HVAC: split units: 66x9000 btu/h, energy class A, SEER>=5, SCOP>=3.8 and 11x12000 btu/h, energy class A, SEER>=5, SCOP>=3.8). • DHW: air-cooled high temperature water heat pump, 68kW and COP>=3.4 energy class>=A. • Lighting:

645677 — SMART GEMS — H2020-MSCA-RISE-2014
D4.3 Lessons learnt from the existing smart / micro grids. Guidelines for scaling-up the existing
infrastructure using mobile connectivity

	• Building Energy Management System: Integrated control system for the energy efficient management of the split type air-conditioning units
Sports facilities / Street Lighting	• DHW: solar thermal collectors • Lighting: 80 x 80W LED
	• 125 x 250W=31.250W • 133 x 125W=16.625W • HQI-E OSRAM 250W • HPI Philips 250W • H125/E27/Kolorlux of General Electric 125W

Figure 3-8 is a schematic of the TUC electrical microgrid. In particular:

- PEM department buildings and University Facilities are powered by two medium to low voltage transformers that operate in an alternate fashion.

- MRED department buildings are connected to the main grid via two medium to low voltage transformers that operate in parallel and simultaneously. Buildings K1 and K2 (old section) of the ENVENG complex are also connected to one of these transformers.

- Electronics and Computer Engineering (ECE) buildings are fed by two medium to low voltage transformers, one of which also provides energy to the new K2 building section, K3 and K4 of the ENVENG department.

- Student dormitories are connected to a separate medium to low voltage transformer.

645677 — SMART GEMS — H2020-MSCA-RISE-2014
D4.3 Lessons learnt from the existing smart / micro grids. Guidelines for scaling-up the existing
infrastructure using mobile connectivity
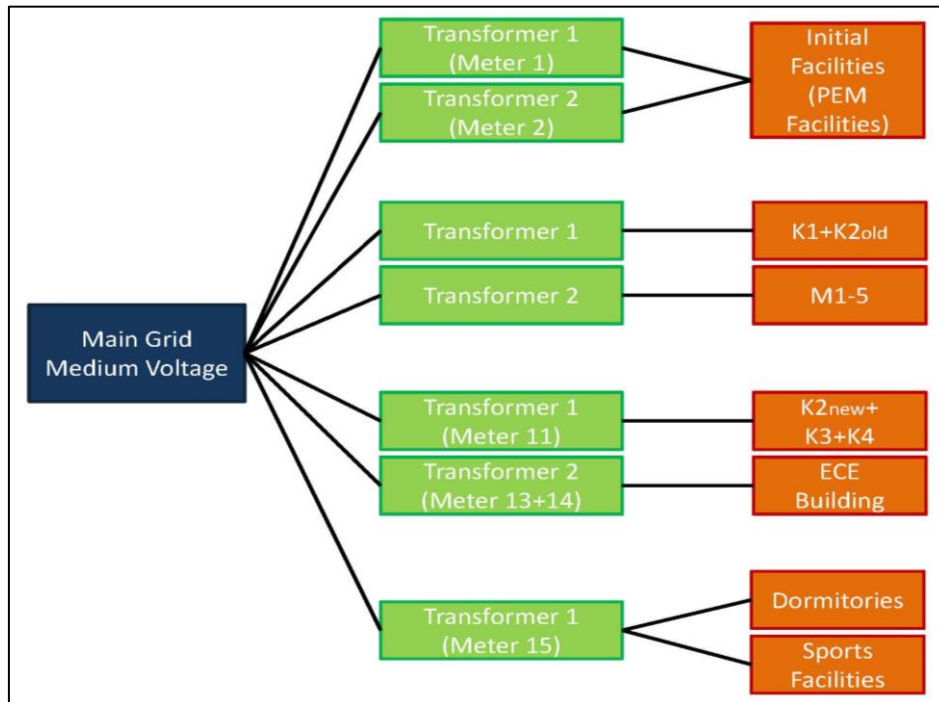
Figure 3-8: Diagram of the electrical power grid at TUC campus

3.2.2 Energy and Power Measurements Data Analysis

Indexes that were used for the data analysis are listed below:

- Peak Power (kW)
- Mean Power (kW)
- Standard Deviation (kW)
- Energy Consumption (kWh)

3.2.3 Load predictions using Artificial Neural Network models

Artificial Neural Network (ANN) models are conceived on the basis of biological nervous systems to imitate information processing and evolution. ANNs assimilate the natural bonds of neurons and their high level interconnection to model complex systems. In the case of predictions ANNs can be more effective compared to statistical, linear or non-linear programming techniques.

ANN models have been used for years in different areas of engineering, science and business to deal with complexity and nonlinearity of data sets. They present capabilities such as adaptive learning, self-organisation, real time operation, fault tolerance and approximation of complex nonlinear functions. ANN modelling is a powerful tool for predicting parameters related to river flows,

645677 — SMART GEMS — H2020-MSCA-RISE-2014
D4.3 Lessons learnt from the existing smart / micro grids. Guidelines for scaling-up the existing
infrastructure using mobile connectivity

wind speed, electricity prices, power production and demand, economic growth, stock market and more [17]–[21].

A typical neural network model consists of three main layers: input, hidden layers and output, as shown in Figure 3-9: The structure of a Back Propagation ANNFigure 3-9.
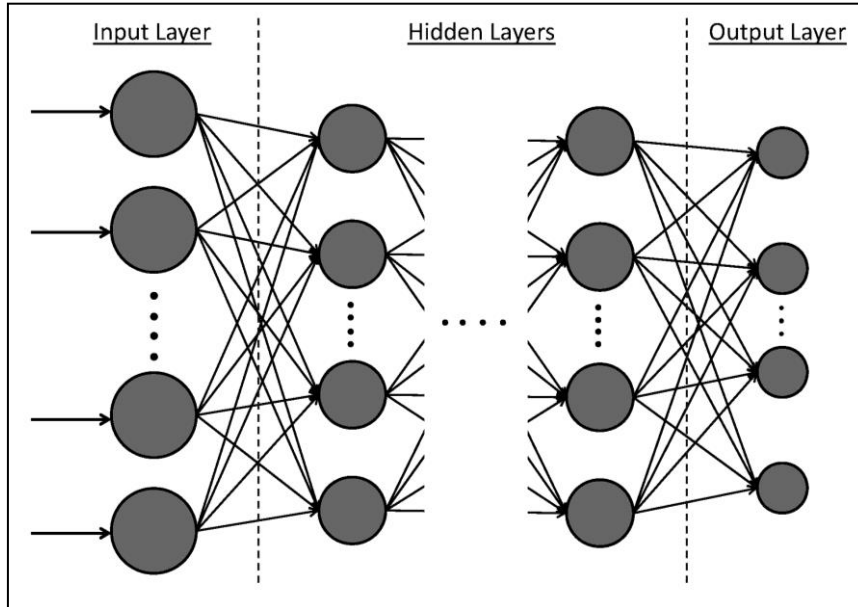
Figure 3-9: The structure of a Back Propagation ANN

Data of meters 1, 3, 6, 8 and 15 was used to predict the power load (kW) of campus facilities in the next 8, 12 and 24 hours. Neural Network Dynamic Time-Series application of Matlab, Nonlinear Autoregressive with External (Exogenous) Input problem definition and Levenberg-Marquardt algorithm for the training process was deployed [20], [22]. The day of the week, hour of the day, and ambient temperature (°C) were used as inputs. Consumed electric power (kW) data was set as target.

3.2.4 Design of PV system at TUC campus

Sunny Design 3 software was used for the modeling of the PV systems. For the PV modules, MPE 250 PS 60 EB (03/2014) with nominal power 250Wp is used connected in series to the STP 150000TL-10 type inverter. In Figure 3-10 and Figure 3-11 technical specifications of the selected PV modules and inverter are provided.

Information on PV modules

The data from the manufacturer's datasheet has been applied. No responsibility is assumed for the correctness of this information.

Manufacturer	Schüco		Cell technology		poly
PV module	MPE 250 PS 60 EB (03/2014)		Certification		EU

Electric properties

		Temperature coefficients		
Nominal power	250.00 Wp	MPP voltage	---	---
Performance tolerance	-0.00/+5.00 W	Open-circuit voltage	-0.3200 %/°C	-119.9 mV/°C
MPP voltage	30.40 V	Short-circuit current	0.0560 %/°C	4.88 mA/°C
MPP current	8.28 A	**Degradation due to aging**		
Open-circuit voltage	37.48 V	Open-circuit voltage tolerance		0.00 %
Short-circuit current	8.71 A	MPP voltage tolerance		0.00 %
Permissible system voltage	1000.00 V	MPP current tolerance		0.00 %
PV module efficiency (STC)	15.28 %	Short-circuit current tolerance		0.00 %
Grounding recommendation	No grounding	**Additional information**		

Mechanical properties

		Additional information	
Number of cells in the PV module	60	Current PV module	Yes
Width	989 mm	Own PV module	No
Length	1654 mm	Favorite	No
Weight	18.20 kg	**Comment**	

Figure 3-10: Information on the selected PV modules

Information on the inverter

Inverter	STP 15000TL-10	Input data	
		Max. DC power	15.34 kW
General data		Max. input voltage	1000 V
Degree of protection	IP65	Rated input voltage	600 V
Width	665 mm	Min. input voltage	150 V
Height	690 mm	Start voltage	188 V
Depth	265 mm	Max. MPP voltage	800 V
Weight	65.0 kg	Max. input current	33.0 A / 11.0 A
Efficiency		Strings per MPP input	5 / 1
Max. efficiency	98.2 %	**Output data**	
European weighted efficiency	97.8 %	Max. AC apparent power	15.00 kVA
		Rated power	15.00 kW
		Min. displacement power factor (value)	0.8
		Nominal AC voltage range	160 - 280 V
		AC power frequency	49.8 - 50.2 Hz
		Feed-in phases	3

Figure 3-11: Information on the selected inverter model

For the better understanding of the relation between the energy production profile of the PV systems and the energy consumption profile of the TUC campus, load matching [23] is determined based on the equation:

$$f_{load,i} = min\left[1, \frac{on\ site\ generation}{load}\right] \times 100\ [\%]$$

Where i is the time interval i.e. hour, day, month.

Scenario 1: 539kWp PV system

In Scenario 1, the PV system configuration consists of 2,156 PV modules and 44 PV inverters. Each inverter is connected to two arrays of 21 PV modules in series each (connected to the 2xA inputs of the inverter) and one array of 7 PV modules in series (connected to the B input of the inverter) as shown in Figure 3-12: Architecture of the PV systemFigure 3-12.
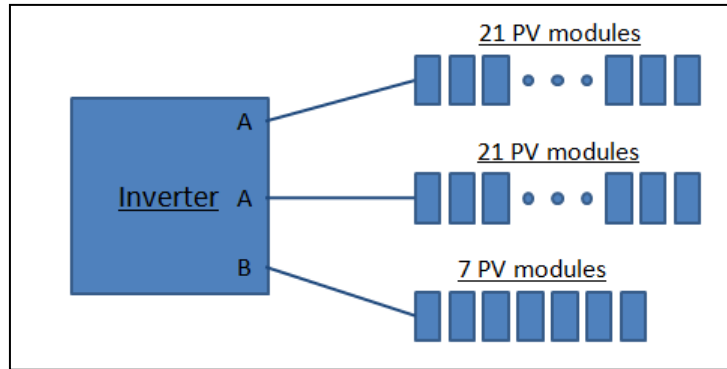
Figure 3-12: Architecture of the PV system

The design considerations related to the compatibility and performance of the proposed PV / inverter configuration and cable losses calculations are presented in Figure 3-13 and Figure 3-14 respectively.
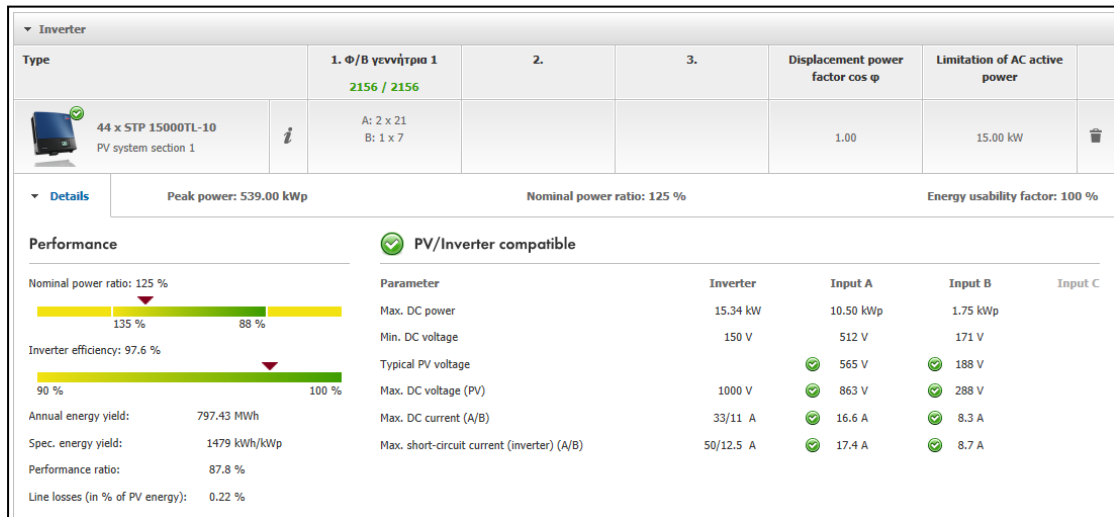
Figure 3-13: The performance of the inverter

645677 — SMART GEMS — H2020-MSCA-RISE-2014
D4.3 Lessons learnt from the existing smart / micro grids. Guidelines for scaling-up the existing
infrastructure using mobile connectivity
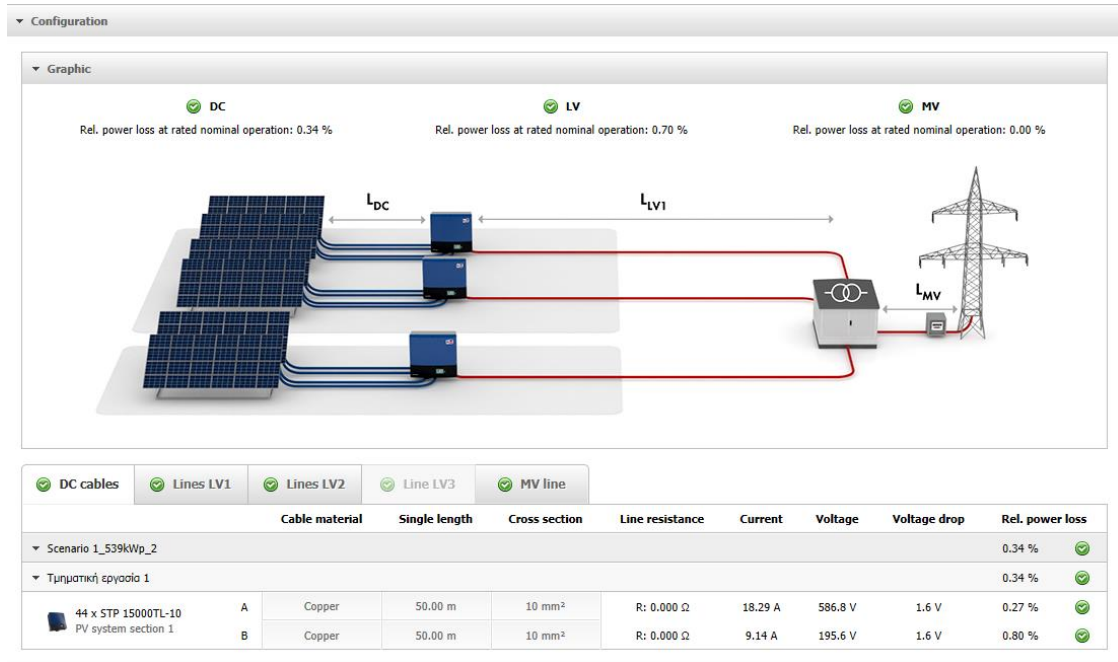
Figure 3-14: The configuration of the system

Scenario 2: 1MWp PV System

In the 2nd scenario the proposed system consists of 4,000 PV modules and 80 PV inverters. The configuration consists of 2 arrays (2 A exits) of 22 PV modules in series each and 1 array (1 B exit) of 6 PV module connected to each inverter as demonstrated in Figure 3-15.
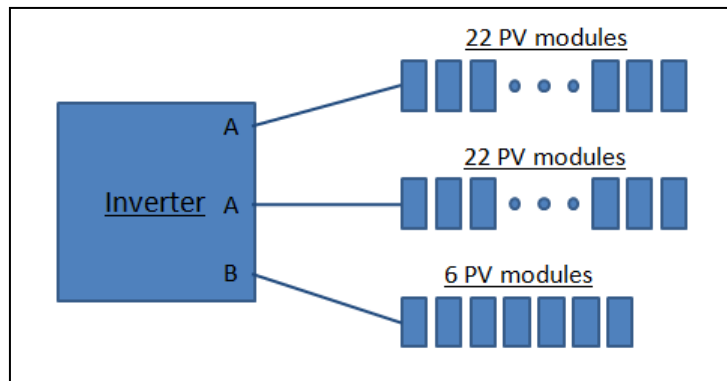
Figure 3-15: Architecture of the PV system

The design considerations of the proposed PV / inverter system including compatibility and performance are presented in Figure 3-16. Cable dimensioning and losses are indicated in Figure 3-17.
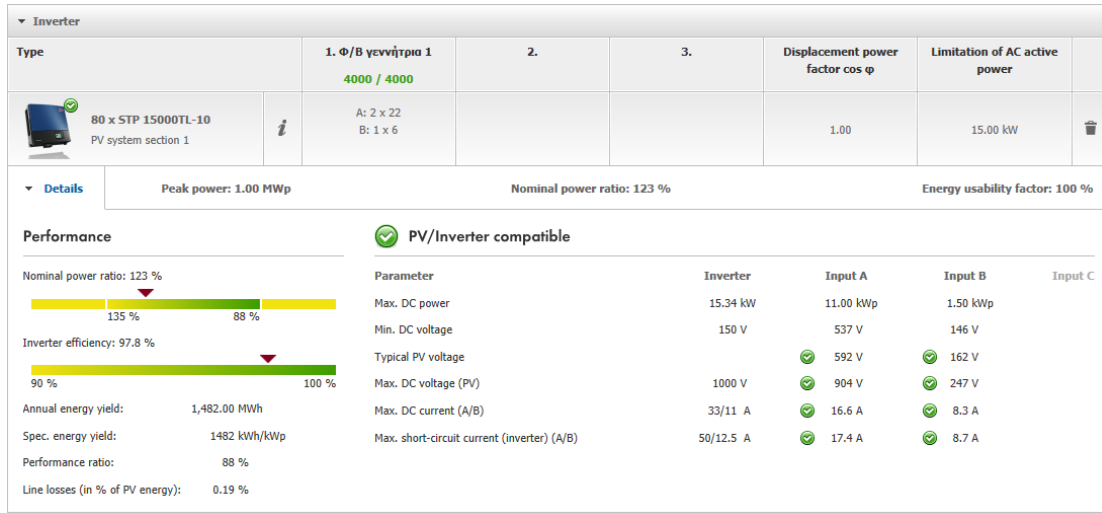
Figure 3-16: The performance of the inverter
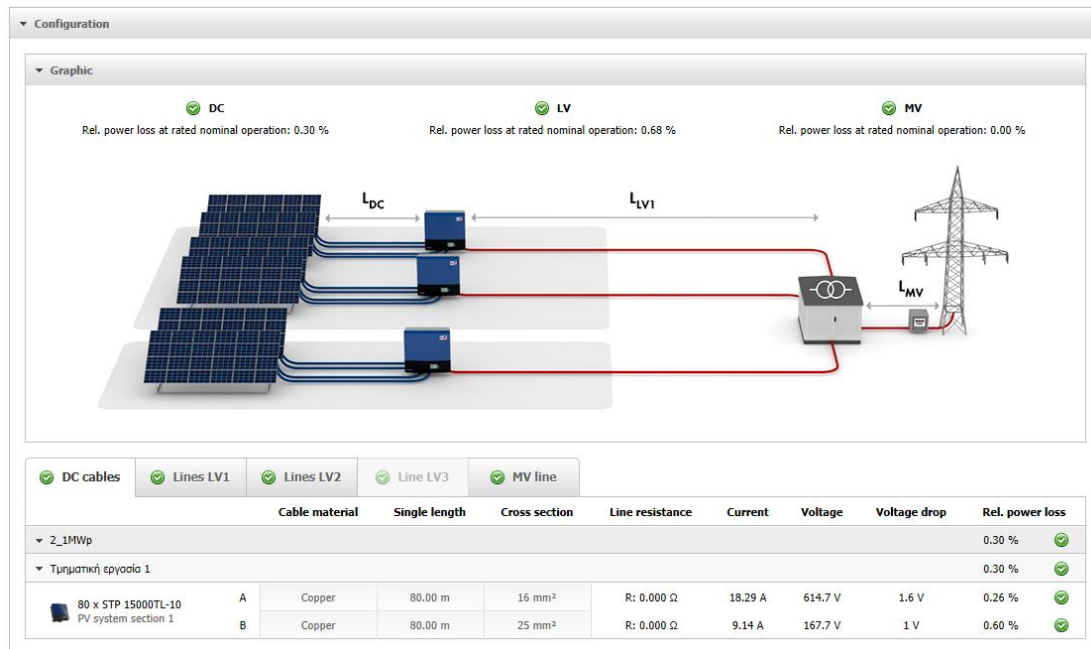
Figure 3-17: The configuration of the system

3.3 Voltage flicker meter design for implementation is smart meters

The universal IEC 61000-4-15 standard provides the functional and design specifications of an analogue or digital flicker measuring device (called Flickermeter) with EMC [24]. According to the IEEE, flicker is defined as "the subjective impression of fluctuating luminance caused by voltage fluctuations", that becomes an annoyance or a disturbance above the defined flicker intensity threshold [25]. The flicker phenomenon i.e. the fluctuating luminance "subjective impression" refers to the variation in illuminance fluctuations disturbance experienced by different individuals at a defined flicker severity, which causes headache, visual tiredness, and could trigger epileptic seizures in individuals diagnosed of epilepsy [24]–[26].

IEC 61000-4-15 standard has been developed through a series of advancements from the conception of the flicker measurement method in the 1980s by UIE, to its 1st publishing in 1992 as IEC 868 standard. IEC 868 defined the short-term flicker severity as the fundamental parameter to evaluate flicker disturbance. The evolution to the most current IEC 61000-4-15 standard published in June 2011 has primary focused on the improvement of results quality from Flickermeter [27]. One gap in the application of IEC Flickermeter based on IEC 61000-4-15 standard is that the incandescent type lamp was used as a reference point in its functional and design specifications at 120 V and 230 V, 50 Hz and 60 Hz voltage and frequency levels. This presents a limitation in the application of IEC Flickermeter to account for the current extensive use of efficient lighting technologies such as LED, CFLs and halogen lamps [24], [27], [28].

IEC 61000-4-15 flickermeter is broken down into the following blocks:

- Block 1 – Input Voltage Adaptor: This constitutes an input signal scaler (that uses an appropriate transducer) with the objective of making flicker severity measurements independent from the input voltage level; it scales the applied amplitude modulated input voltage $u(t)$ to modulated RMS voltage, V_{RMS}, and then sampled using analogue-to-digital converter that regulates the modulated V_{RMS} level to the constant voltage reference value V_R. [24], [29], [30].

- Block 2 – Squaring multiplier: This is a demodulator that recovers voltage fluctuation by squaring the output of block 1 (V_{RMS} – scaled in block 1 from $u(t)$ to a reference level V_R in order to simulate the correct behaviour of an incandescent [24], [29], [30].

- Block 3 – Weighing filters: This part of the circuit is responsible for the eye response simulation to an incandescent lamp consisting of three cascaded filters, with a range selector for sensitivity measurement. The first two consecutive filters are part of the demodulation process/system, namely 1st-order high-pass filter with a 3 dB cut-off frequency of 0.05Hz, and 6th-order low-pass Butterworth filter with a 3 dB cut-off frequency of 35Hz (implemented as three cascades of second-order filter). The third also referred to as the weighting filter models the lamp-eye system [24], [29], [30].

- Block 4 – Squaring and smoothing: This models the eye-brain system and low-pass filter that simulates the eye-brain response and perceptual storage effect of flickering in the human brain. The output P_{inst} of this block is obtained by squaring the output of block 3 filtered using a 1st-order low pass filter at $t = 0.3$ s [24], [29], [30].

- Block 5 – Online statistical analysis: A statistical approach is deployed to evaluate P_{st}. P_{inst} is normalised to evaluate P_{st} for a time period of $T_{short} = 10$ min "when a sine wave-modulated 50 Hz input signal, with a modulation frequency of 8.8 Hz and a modulation depth of 0.25% (Voltage fluctuation $\Delta U/U$, %), is applied" [29].

645677 — SMART GEMS — H2020-MSCA-RISE-2014
D4.3 Lessons learnt from the existing smart / micro grids. Guidelines for scaling-up the existing
infrastructure using mobile connectivity
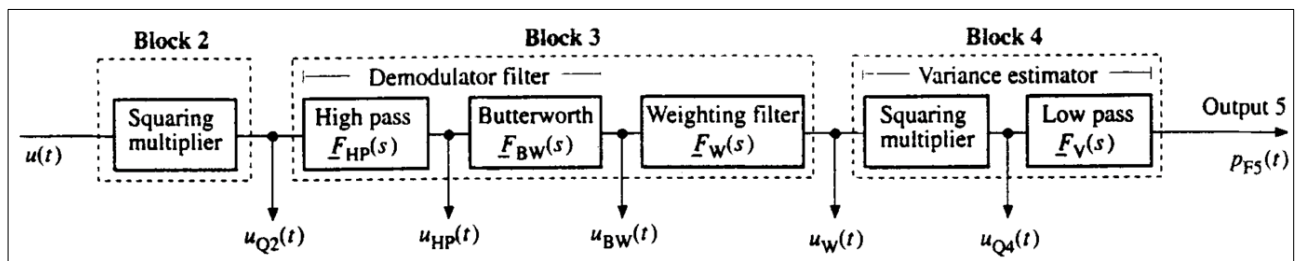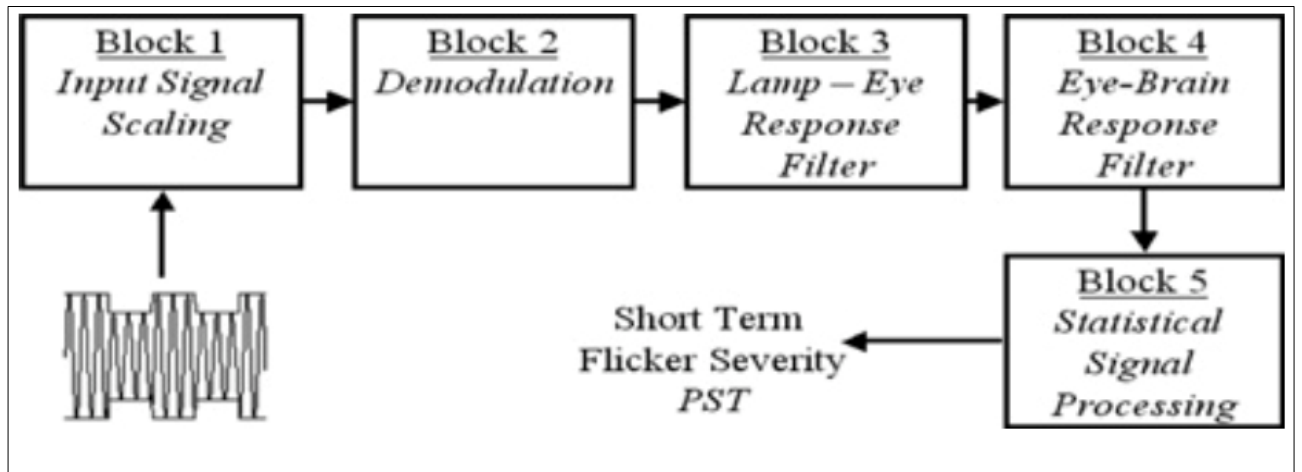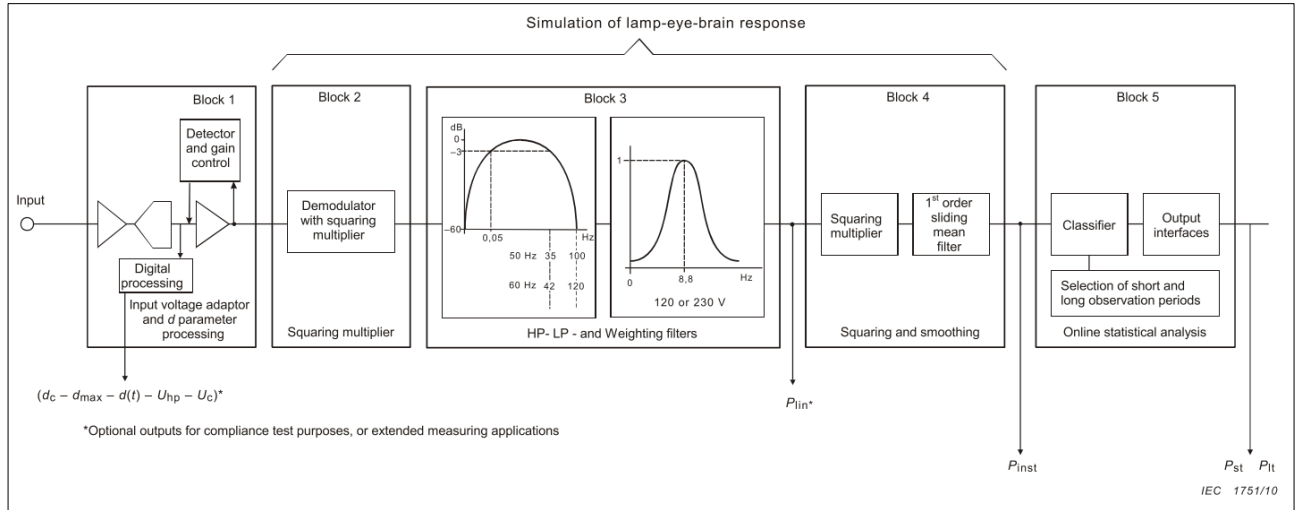
Figure 3-18: "Functional diagram of IEC Flickermeter" [24], "IEC 61000-4-15 Flickermeter block diagram" [29] and "Signal flow diagram of the IEC Flickermeter (block 1 and block 5 are not necessary for the calculation) [31]

The methodology for evaluating the flicker intensity is defined by the two performance indicators listed below:

- Short-term severity (P_{st}): P_{st} is applicable in the evaluation of individual source disturbance characterised by short-duty cycle such as rolling mills, residential domestic appliances etc. Unless otherwise specified, P_{st} is

645677 — SMART GEMS — H2020-MSCA-RISE-2014
D4.3 Lessons learnt from the existing smart / micro grids. Guidelines for scaling-up the existing
infrastructure using mobile connectivity

usually measured over 10 min period (T_{short}). Different time intervals may be used when carrying out case-studies or surveys on power quality. The formula used to evaluate P_{st} for a time period of T_{short} is derived from time-at-level statistics, where the suffix "s" specifies the use of smoothed values in block 4 of the IEC Flickermeter (see Figure 3-18) [24], [30]:

$$P_{st} = \sqrt{0.0314P_{0.1} + 0.0525_{1s} + 0.0657P_{3s} + 0.28P_{10s} + 0.08P_{50s}}$$
(Eq. 1)

The above formula is obtained from block 5 classifier of a functional IEC Flickermeter (see Figure 3-18). The indication of exceeded flicker level for 0.1%, 1%, 3%, 10% and 50% during the period of observation are represented by percentiles variable $P_{0.1}, P_1, P_3, P_{10}$ and P_{50} respectively. The formulas of these variables are presented below [24]:

$$P_{50s} = (P_{30} + P_{50} + P_{80})/3 \text{ (Eq. 2)}$$
$$P_{10s} = (P_6 + P_8 + P_{10} + P_{13} + P_{17})/3 \text{ (Eq. 3)}$$
$$P_{3s} = (P_{2.2} + P_3 + P_4)/3 \text{ (Eq. 4)}$$
$$P_{1s} = (P_{0.7} + P_1 + P_{1.5})/3 \text{ (Eq. 5)}$$

- Long-term severity (P_{lt}): P_{lt} is applicable in the evaluation of combined effect of multiple disturbances characterised with long and variable duty cycle such as arc furnaces. Unless otherwise specified, P_{lt} is usually measured over 2 h period ($T_{long} = N\,T_{short}$, where $N = 12$), The formula used to evaluate P_{lt} for a time period of $T_{long} = 2$ h is [24], [30]:

$$P_{lt} = \sqrt[3]{\frac{\sum_{i=1}^{N} P_{st_i}^3}{N}} \text{ (Eq. 6)}$$

Note: P_{st_i} are successive readings of P_{st} for $I = 1, 2, 3…$[24].

3.3.1 Infinite Impulse Response Filter Design
Problem Definition

IIR filter with the input-output relationship is modelled by (Eq. 7, with a transfer function described by (Eq. 8 [32].

645677 — SMART GEMS — H2020-MSCA-RISE-2014
D4.3 Lessons learnt from the existing smart / micro grids. Guidelines for scaling-up the existing
infrastructure using mobile connectivity

$$y(n) = -\sum_{k=1}^{M} b(k)\, y(n-k) + \sum_{k=0}^{N} a(k)\, x(n-k) \quad \text{(Eq. 7)}$$

where $y(n)$ is the IIR filter's output and $x(n)$ is the IIR filter's input

The equation is re-arranged to take the following form;

$$\sum_{k=0}^{M} b(k)\, y(n-k) = \sum_{k=0}^{N} a(k)\, x(n-k)$$

$$\text{with } b(0) = 1, \sum_{k=1}^{M} b(k)\, [z^{-k} y(n)] = \sum_{k=0}^{N} a(k)\, [z^{-k} x(n)]$$

where z^{-k} is considered as a unit delay operator, i.e. a delay of one sample interval.

$$\therefore\; z^{-k} x(n) = x(n-k)$$

Therefore, the transfer function in terms of z is:

$$H(z) = \frac{y(n)}{x(n)} = \frac{\sum_{k=0}^{N} a(k) z^{-k}}{\sum_{k=0}^{M} b(k) z^{-k}} = \frac{a(0) + a(1)z^{-1} + \cdots + a(N)z^{-N}}{1 + b(1)z^{-1} + b(2)z^{-2} + \cdots + b(M)z^{-M}} \quad \text{(Eq. 8)}$$

where $H(z)$ is the digital transfer function, $a(k)$ and $b(k)$ are the filter coefficients

Therefore, the aim of this section is to evaluate all filter coefficients in block 3 and block 4.

3.3.2 Bilinear Transformation Method

The term bilinear refers to the fact that the numerator and denominator of the transformation equation are linear in form. Bilinear transformation method also referred to as the bilinear z-transform is carried out via change of variables given in (Eq. 9. It uses frequency domain method to transform analogue filter transfer function *H(s)* to digital transfer function *H(z)* [32].

$$s = \frac{2}{T}\frac{(z-1)}{(z+1)} = 2f_S\frac{(z-1)}{(z+1)} \quad \text{(Eq. 9)}$$

where *s* is the Laplace complex variable, and *z* is a complex variable, hence giving rise to complex polynomials of *H(z)* where digital frequency response can be obtained [32].

$$z = e^{j\omega T} \quad \text{(Eq. 10)}$$

645677 — SMART GEMS — H2020-MSCA-RISE-2014
D4.3 Lessons learnt from the existing smart / micro grids. Guidelines for scaling-up the existing
infrastructure using mobile connectivity

where ω is the digital frequency response.

The relationship between analogue and digital frequencies is governed by (Eq. 11 below [32]:

$$\omega' = \frac{2}{T} \tan\left(\frac{\omega T}{2}\right) \quad \text{(Eq. 11)}$$

where

$\omega' is\ the$ analogue frequency response and $\omega\ is\ the$ digital frequency response

Figure 3-19 is a frequency warping graph that describes the relationship between ω' and ω; it shows an approximate linear relationship and non-linear relationship for small values of ω, and increasing values (higher values) of ω respectively. This non-linearity leads to warping (or distortion) of ω'. Also, Figure 3-19 shows three passbands of constants width and regular spacing for ω, and unequal width and irregular spacing after the application of bilinear transformation [32].
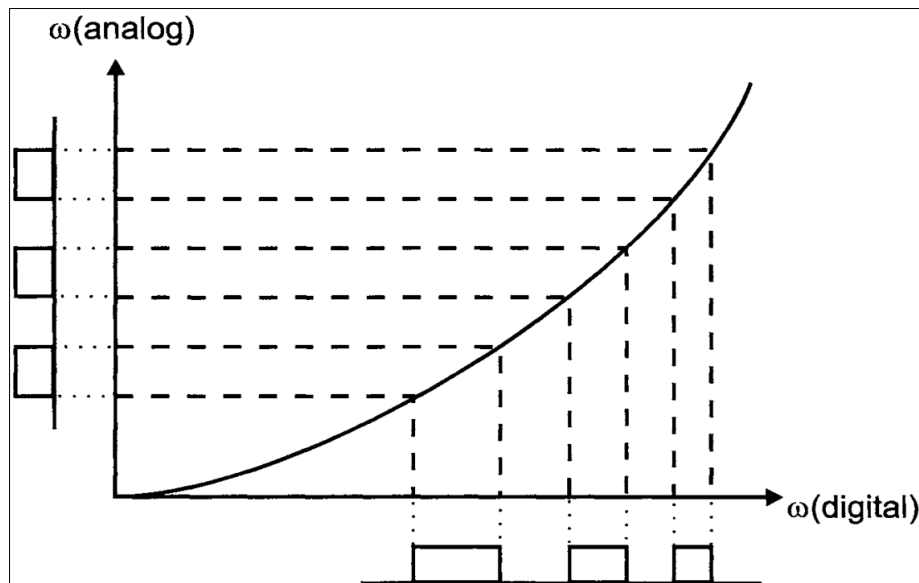
Figure 3-19: Frequency warping (or distortion) [32]

This distortion effect can be corrected via pre-warping (or scaling) of the analogue filter (analogue frequency scaling) by making *s* equivalent to *sK* (where "*K* is some constant"). The required pre-warping is defined by (Eq. 12 [32];

$$u_0 = \frac{2}{T} \tan\left(\frac{T\omega_0}{2}\right) \quad \text{(Eq. 12)}$$

645677 — SMART GEMS — H2020-MSCA-RISE-2014
D4.3 Lessons learnt from the existing smart / micro grids. Guidelines for scaling-up the existing
infrastructure using mobile connectivity

where u_0 *is the* critical frequency of the analogue filter, and ω_0 *is the* desired critical frequency of the digital filter.

Pre-warping with bilinear transformation is defined in (Eq. 13 [32];

$$u_0 = \frac{2K}{T} \tan\left(\frac{T\omega_0}{2}\right) \text{ (Eq. 13)}$$

(Eq. 14 is then derived by substituting (Eq. 9 in terms of 2/T into (Eq. 13 ;

$$\therefore u_0 = \frac{s\,(z+1)\,K}{(z-1)} \tan\left(\frac{T\omega_0}{2}\right)$$

$$sK \approx s = \frac{u_0}{\tan\left(\frac{T\omega_0}{2}\right)} \frac{(z-1)}{(z+1)} = \alpha \frac{(z-1)}{(z+1)} \ (note: \alpha = \frac{u_0}{\tan\left(\frac{T\omega_0}{2}\right)}) \text{ (Eq. 14)}$$

3.3.3 IEC Flickermeter Filter Transfer Functions

The filter design and implementation is based on [31], [33], [34], [35].

Block 3 – 1st-Order High Pass Filter

Analogue frequency response of the 1st-order high pass filter with a 3dB cut-off frequency f_c of 0.05Hz is govern by (Eq. 15:

$$F_{HP_{1st}}(s) = \frac{s\tau}{1+ s\tau} = \frac{s/\omega_c}{1+ s/\omega_c} \text{ (Eq. 15)}$$

where $\omega_c = 2\pi f_c = 2\pi 0.05\ s^{-1}, \tau = \frac{1}{2\pi 0.05} = 3.1831\ s, f_s = 100\ Hz$

(Eq. 16 governs transfer function in the z-domain, obtained by applying bilinear transformation method:

$$H_{HP_{1st}}(z) = \frac{y(n)}{x(n)} = \frac{\sum_{k=0}^{N} a(k)z^{-k}}{\sum_{k=0}^{M} b(k)z^{-k}} = \frac{a(0) + a(1)z^{-1}}{1+b(1)z^{-1}} = C \frac{1+ az^{-1}}{1+ bz^{-1}} \text{ (Eq. 16)}$$

where $C = \frac{2\pi f_S}{(1+ 2\pi f_S)}$, $a = -1, b = \frac{(1- 2\pi f_S)}{(1+ 2\pi f_S)}$ and f_s is the sampling rate

$$\therefore H_{HP_{1st}}(z) = \frac{\left(\frac{2\pi f_S}{1+ 2\pi f_S}\right) - \left(\frac{2\pi f_S}{(1+ 2\pi f_S)}\right) z^{-1}}{1 + \left(\frac{(1- 2\pi f_S)}{(1+ 2\pi f_S)}\right) z^{-1}}$$

Therefore, the 1st-order high pass filter is represented by differential equations (Eq. 17:

$$y(n) = \left(\frac{2\pi f_S}{1+ 2\pi f_S}\right) - \left(\frac{2\pi f_S}{(1+ 2\pi f_S)}\right) z^{-1}$$

$$y_n = -b(1)y(n-1) + a(0)x(n) + a(1)(x-1) \text{ (Eq. 17)}$$

645677 — SMART GEMS — H2020-MSCA-RISE-2014
D4.3 Lessons learnt from the existing smart / micro grids. Guidelines for scaling-up the existing
infrastructure using mobile connectivity

$$\therefore y_n = -\left(\frac{(1 - 2\pi f_S)}{(1 + 2\pi f_S)}\right)y(n-1) + \left(\frac{2\pi f_S}{1 + 2\pi f_S}\right)x(n) - \left(\frac{2\pi f_S}{(1 + 2\pi f_S)}\right)x(n-1)$$

Table 3-2: 1st-order high pass filter coefficients for G3G balance meters to be implemented in 230V lamp based on sampling frequency of 100 Hz

1st-order high pass filter coefficients	Formula	Values
a_0	$\left(\dfrac{2\pi f_S}{1 + 2\pi f_S}\right)$	0.99841
a_1	$-\left(\dfrac{2\pi f_S}{(1 + 2\pi f_S)}\right)$	-0.99841
b_1	$\dfrac{(1 - 2\pi f_S)}{(1 + 2\pi f_S)}$	-0.99682

Block 3 – 6th-Order Low Pass Butterworth Filter

Analogue frequency response of the pre-warp 6th-order Butterworth low pass filter is given by (Eq. 18:

$$F_{BW_{6th}}(s) = \frac{1}{\sum_{i=1}^{6} a_i \left(\frac{s}{\omega_c'}\right)^i} \text{ (Eq. 18)}$$

where $\omega_c = 2\pi f_c = 2\pi 35 \ s^{-1}$ and $\omega_c' = \tan\left(\frac{w_c}{2f_S}\right)$

(Eq. 19 governs transfer function in the z-domain, obtained by subdividing the filter into 3 cascades of 2nd-order filters and applying bilinear transformation method:

$$H_{BW_{6th}}(z) = C \prod_{k=1}^{3} \frac{a_{ok} + a_{1k}z^{-1} + a_{2k}z^{-2}}{1 + bz^{-1} + b_{2k}z^{-2}} \text{ (Eq. 19)}$$

Therefore, the 6th-order Butterworth low pass filter is represented by 3 differential equations ((Eq. 20, (Eq. 21, and (Eq. 22):

$$y_{n,1} = A_1\left(x_{n,1} + 2x_{n-1,1} + x_{n-2,1}\right) - B_1 y_{n-1,1} - D_1 y_{n-2,1} \text{ (Eq. 20)}$$

$$y_{n,2} = E_2\left(x_{n,2} + 2x_{n-1,2} + x_{n-2,2}\right) - F_2 y_{n-1,2} - G_2 y_{n-2,2} \text{ (Eq. 21)}$$

$$y_{n,3} = H_3\left(x_{n,3} + 2x_{n-1,3} + x_{n-2,3}\right) - I_3 y_{n-1,3} - J_3 y_{n-2,3} \text{ (Eq. 22)}$$

$$\therefore y_n = (y_{n,1})(y_{n,2})(y_{n,3})$$

where,

$$R = \tan(f_c \pi / f_s) = 1.96261 \ rad, \theta_i = \frac{\pi(5 + 2i)}{12} = , f_c = 35 Hz, and \ f_s = 100 \ Hz$$

645677 — SMART GEMS — H2020-MSCA-RISE-2014
D4.3 Lessons learnt from the existing smart / micro grids. Guidelines for scaling-up the existing
infrastructure using mobile connectivity

Table 3-3: 6th-order Butterworth low pass filter coefficients for G3G balance meters to be implemented in 230V lamp based on sampling frequency of 100 Hz

Weighing filter coefficients	Formulas for θ_i	Formulas for coefficients	Values
A_1	$\theta_1 = \dfrac{\pi(5 + 2 \times 1)}{12}$ $= 1.83260$	$A_1 = \dfrac{R^2}{1 + R^2 - 2R\cos\theta_1}$	0.65644
B_1	$\theta_1 = \dfrac{\pi(5 + 2 \times 1)}{12}$ $= 1.83260$	$B_1 = \dfrac{2(R^2 - 1)}{1 + R^2 - 2R\cos\theta_1}$	0.97203
D_1	$\theta_1 = \dfrac{\pi(5 + 2 \times 1)}{12}$ $= 1.83260$	$D_1 = \dfrac{1 + R^2 + 2R\cos\theta_1}{1 + R^2 - 2R\cos\theta_1}$	0.65372
E_2	$\theta_2 = \dfrac{\pi(5 + 2 \times 2)}{12}$ $= 2.35619$	$E_2 = \dfrac{R^2}{1 + R^2 - 2R\cos\theta_2}$	0.50500
F_2	$\theta_2 = \dfrac{\pi(5 + 2 \times 2)}{12}$ $= 2.35619$	$F_2 = \dfrac{2(R^2 - 1)}{1 + R^2 - 2R\cos\theta_2}$	0.74779
G_2	$\theta_2 = \dfrac{\pi(5 + 2 \times 2)}{12}$ $= 2.35619$	$G_2 = \dfrac{1 + R^2 + 2R\cos\theta_2}{1 + R^2 - 2R\cos\theta_2}$	0.27222
H_3	$\theta_2 = \dfrac{\pi(5 + 2 \times 3)}{12}$ $= 2.87979$	$H_3 = \dfrac{R^2}{1 + R^2 - 2R\cos\theta_3}$	0.44564
I_3	$\theta_2 = \dfrac{\pi(5 + 2 \times 3)}{12}$ $= 2.87979$	$I_3 = \dfrac{2(R^2 - 1)}{1 + R^2 - 2R\cos\theta_3}$	0.65990
J_3	$\theta_2 = \dfrac{\pi(5 + 2 \times 3)}{12}$ $= 2.87979$	$J_3 = \dfrac{1 + R^2 + 2R\cos\theta_3}{1 + R^2 - 2R\cos\theta_3}$	0.12268

Block 3 – Weighing Filter

Analogue frequency response of the weighing filter is provided by (Eq. 23:

$$F_{WF}(s) = \frac{k\omega_1 s}{s^2 + 2\lambda s + \omega_1^2} \times \frac{1 + s/\omega_2}{(1 + s/\omega_3)(1 + s/\omega_4)} \text{ (Eq. 23)}$$

(Eq. 24 and (Eq. 25 define the transfer function in the z-domain, obtained by subdividing the weighting filter into two filters of second order and the bilinear transformation method:

$$H_{WF1}(z) = \frac{a - az^{-2}}{b + cz^{-1} + dz^{-2}} \text{ (Eq. 24)}$$

645677 — SMART GEMS — H2020-MSCA-RISE-2014
D4.3 Lessons learnt from the existing smart / micro grids. Guidelines for scaling-up the existing
infrastructure using mobile connectivity

$$H_{WF2}(z) = \frac{e + 2z^{-1} + fz^{-2}}{g + hz^{-1} + Lz^{-2}} \quad \text{(Eq. 25)}$$

where $f_s = 100\ Hz, N_1 = 4f_s^2 + 4\lambda f_s + w_1^2$, and $N_2 = 1 + \frac{2f_s}{\omega_3} + \frac{2f_s}{\omega_4} + \frac{4f_s^2}{\omega_3 \omega_4}$

Therefore, the weighting filter is represented by two differential equations ((Eq. 26 and (Eq. 27):

$$y_{n,1} = A(x_{n,1} - x_{n-2,1}) - By_{n-1,1} - Dy_{n-2,1} \quad \text{(Eq. 26)}$$

$$y_{n,2} = Ex_{n,2} + Fx_{n-1,2} + Gx_{n-2,2} - Iy_{n-1,2} - Jy_{n-1,2} \quad \text{(Eq. 27)}$$

$$\therefore y_n = (y_{n,1})(y_{n,2})$$

Table 3-4: Constant values for the 230V incandescent lamp [24]

Variable	230V lamp
k	1.74802
λ	2π4.05981
ω_1	2π9.15494
ω_2	2π2.27979
ω_3	2π1.22535
ω_4	2π21.9

Table 3-5: Weighing filter coefficients for G3G balance meters to be implemented in 230V lamp based on sampling frequency of 100 Hz

Weighing filter coefficients	Formulas	Values
A	$A = \dfrac{2kw_1 f_s}{N_1}$	0.37580
B	$B = \dfrac{2w_1^2 - 8f_s^2}{N_1}$	-1.37132
D	$D = \dfrac{4f_s^2 - 4\lambda f_s + w_1^2}{N_1}$	0.61865
E	$E = \dfrac{1 + 2\dfrac{f_s}{\omega_2}}{N_2}$	0.22606
F	$F = \dfrac{2}{N_2}$	0.030217
G	$G = \dfrac{1 - 2\dfrac{f_s}{\omega_2}}{N_2}$	-0.19584
I	$I = \dfrac{2 - \dfrac{8f_s^2}{\omega_3 \omega_4}}{N_2}$	-1.11069

645677 — SMART GEMS — H2020-MSCA-RISE-2014
D4.3 Lessons learnt from the existing smart / micro grids. Guidelines for scaling-up the existing
infrastructure using mobile connectivity

J	$J = \dfrac{1 - \dfrac{2f_s}{\omega_3} - \dfrac{2f_s}{\omega_4} + \dfrac{4f_s{}^2}{\omega_3\omega_4}}{N_2}$	0.17113

Block 4 – 1st-Order Low Pass Filter

Analogue frequency response of the 1st-order low pass filter is given by (Eq. 28:

$$F_{HP_{1st}}(s) = \frac{s}{1+s\tau} = \frac{s}{1+s/\omega_c} \quad \text{(Eq. 28)}$$

(Eq. 29 governs the transfer function in the z-domain, obtained by applying bilinear transformation method:

$$H_{HP_{1st}}(z) = \frac{y(n)}{x(n)} = \frac{\sum_{k=0}^{M} a(k)z^{-k}}{\sum_{k=0}^{N} b(k)z^{-k}} = \frac{a(0) + a(1)z^{-1}}{1 + b(1)z^{-1}} = C\frac{1 + z^{-1}}{1 + bz^{-1}} \quad \text{(Eq. 29)}$$

where $C = \dfrac{f_c}{f_c + 1}$, $f_s = 100\ Hz$, $f_c = \dfrac{1}{2\pi f_s} = 0.0015915$ and $a = \dfrac{f_c - 1}{f_c + 1}$

$$\therefore H_{LP_{1st}}(z) = \frac{\left(\dfrac{f_c}{f_c + 1}\right) + \left(\dfrac{f_c}{f_c + 1}\right)z^{-1}}{1 + \left(\dfrac{f_c - 1}{f_c + 1}\right)z^{-1}}$$

Therefore, the 1st-order low pass filter is represented by differential equations (Eq. 30:

$$y_n = y_n = -b(1)y(n-1) + a(0)x(n) + a(1)(x - 1) \quad \text{(Eq. 30)}$$

$$\therefore y_n = -\left(\frac{f_c - 1}{f_c + 1}\right)y(n-1) + \left(\frac{f_c}{f_c + 1}\right)x(n) + \left(\frac{f_c}{f_c + 1}\right)x(n-1)$$

Table 3-6: 1st-order low pass filter coefficients for G3G balance meters to be implemented in 230V lamp based on sampling frequency of 100 Hz

1st-order low pass filter coefficients	Formulas	Values
a_0	$\left(\dfrac{f_c}{f_c + 1}\right)$	0.0015890
a_1	$\left(\dfrac{f_c}{f_c + 1}\right)$	0.0015890
b_1	$\left(\dfrac{f_c - 1}{f_c + 1}\right)$	-0.99682

3.4 Testing of smart meter communication, authentication and encryption protocols

According to the European Commission report [36] an estimation of 200 million smart meters for electricity (representing approximately 72% of all European consumers) will be installed by 2020. The smart meters providers must ensure that the meters cannot be tempted either by physical or electronic means because this will result in huge economic damage to electricity utilities companies. Smart meters rely on deferent protocol for communicate with the utilities companies to send or receive commands (i.e. remote disconnection from the grid) and data (billing information). A crucial part of this procedure is the authentication of the utility company when it tries to connect to the smart meters using the various communication protocols available. A framework will be developed for testing various methods to attack the authentication procedure and try to gain unauthorized access to the smart meters. This framework will be used to verify any new version of the software installed on the smart meters will be secured by unauthorized access via the carious communication protocols.

3.4.1 Smart metering communication protocols

The DLMS/COSEM protocol used by various Smart Meters for communication purposes with the concentrator. DLMS stands for Device Language Message Specification and consists of a general concept for abstract modeling of communication entities. On the other hand, COSEM is derived from the Companion Specification for Energy Metering. It includes a set of standards that defines the rules for data exchange between devices, such as an energy meter and a data accumulator. Together they enable several features, such as (a) an object model to view and access the different functionalities of a meter, (b) an identification system for all data, (c) a method for communicating with the model and (d) a transport layer to accommodate the information flows between the meter and other devices. The official website of the DLMS User association and provides a simple introduction to the protocol. Registered members may also obtain the complete DLMS/COSEM specification, also known as the colored books, namely:

645677 — SMART GEMS — H2020-MSCA-RISE-2014
D4.3 Lessons learnt from the existing smart / micro grids. Guidelines for scaling-up the existing
infrastructure using mobile connectivity

- Blue book: COSEM meter object model and the OBIS (OBject Identification System) codes[37]
- Green book: describes the different architecture and protocols [37]
- Yellow book: describes requirements and procedures for conformance testing. [37]
- White book: glossary of terms for DLMS/COSEM [37]

The protocol is based on the OSI (Open System Interconnection) seven layer model. However they are collapsed in four:

- physical: defines how to transfer information to and from the meter
- data link: provides the messaging methods to modify data and communicate with the device
- transport: enables data transfer based various interfaces
- application layers: represents the functional aspects of the energy meter so applications can access them

Prior to exchanging metering information an association must be set up, initiated by the client, through the object model interface. From that moment the server is also able to send notifications without explicit request.

Clock synchronization and transmission of measurement profiles are also features of DLMS/COSEM. Finally, it includes authentication and confidentiality services based on symmetric key encryption.

In DLMS/COSEM the communication model follows the server/client paradigm. The meter acts as a server, and replies to the client's application requests to retrieve data, change configurations, perform specific actions, etc.

Prior to gaining access to the COSEM objects in the server, both parties, client and server, need to define the context, which includes:

- the application context.
- the authentication context.
- the xDLMS context.

xDLMS stands for extended DLMS and is an extension of the DLMS protocol, with emphasis on metering applications.

The exchange of this information is called an application association (AA). Depending on the AA, different access rights may be granted by the server. Permissions can be defined with respect to object visibility but also with access

645677 — SMART GEMS — H2020-MSCA-RISE-2014
D4.3 Lessons learnt from the existing smart / micro grids. Guidelines for scaling-up the existing
infrastructure using mobile connectivity

to specific attributes and methods. To that extent, the complete list of visible objects can be retrieved by the client and is called association view.

In order to enforce access rights, DLMS/COSEM defines security policies for the access and transport of data. Access controls restrict access to the data stored in the meter. While data transport pertains to the use of cryptography to protect the data in transit. Ideally, only the parties with the necessary keys can then decrypt the data and obtain access to the original content, the plain text.

Access to data can be restricted in DLMS/COSEM. Therefore metering equipment must authenticate the clients to ensure they are only awarded access to the data they have permission. The authentication context is negotiated between client and server at the AA stage.

 DLMS/COSEM supports three categories of data access protection:

- Lowest level security (no security).

- Low Level Security (LLS): requires the use of a password. The server is not authenticated by the client

- High Level Security (HLS): provides mutual (client and server) authentication

In both LLS and HLS the authentication takes place during the AA. The HLS authentication process involves four steps that consist of exchanging challenges and inspecting the results with cryptographic methods.

The HLS security context is indicated for all situations where no protection of the data communication channels is expected. This mode can use four different algorithms, MD5, SHA-1, GMAC (Galois Message Authentication Code) or a secret method known only by the meter and the client. For our case the GMAC [38] algorithm is used.

In addition to client authentication, the data transport can be encrypted. These protections are applied to APDUs to ensure they cannot be deciphered on transit. The security policies available for data transport are:

• No security.

• Authentication.

• Encryption.

• Authentication and encryption.

For our case the authentication and encryption mode is used.

645677 — SMART GEMS — H2020-MSCA-RISE-2014
D4.3 Lessons learnt from the existing smart / micro grids. Guidelines for scaling-up the existing
infrastructure using mobile connectivity

3.4.2 Fuzzing

Fuzzing [39] is an automated software testing technique, without access to the source code of the target, to uncover vulnerabilities through testing. This is done providing invalid, unexpected or random data as input to the computer program/device. The program/device is monitoring during the course of the test for exception like crashed, reboots, halts, delay in execution or memory leaks.

The aim of the current research is to examine the implementation of the DLMS/COSEM protocol for the optical port (Figure 3-20) that is found on most of the smart meters, part of the physical layer. The communication device (seen attached to the meter: Figure 3-21) can be connected to any PC and it is essential a Serial to USB converter.

Figure 3-20 Reference smart meter

The reference smart meter is the GAMA 300, part of the line of smart meter by Elgama Electronica. It is an accurate single/three phase electricity meter with communication capabilities: optical, Power Line Communication (PLC) [40] , wireless or wired MBus [41], RS485, Ethernet.

645677 — SMART GEMS — H2020-MSCA-RISE-2014
D4.3 Lessons learnt from the existing smart / micro grids. Guidelines for scaling-up the existing
infrastructure using mobile connectivity

Figure 3-21 Reference smart meter with optical communication device

4. Guidelines for scaling-up the existing infrastructure using mobile connectivity

Scaling-up the existing infrastructure is possible by establishing the proper interventions leading to higher energy efficiency and cost savings. This can be achieved by following a coherent analysis and implementation of technological and scientific advances. Transition to a near zero energy district requires effective technological measures to be applied in building and district level and be supported by organisational measures and active user engagement. Guidelines and lessons learnt through the staff exchange and the related work performed in this phase are listed below:

- Distributed analytic measurements of power consumption and production are a prerequisite for understanding the operational performance of settlements and identify performance gaps or areas for improvement.

- Smart metering installations needs to follow specific rules which vary according to the application. District level smart metering needs to be hierarchical and provide ways to ensure the validity and reproduction of missing or corrupt data.

- Smart monitoring needs to be easily accessible by authorised users and promote engagement by simple, accurate and valid representation of the parameters in the branch or installation under investigation.

- Processing of measurements should be straightforward while avoiding vagueness, data conflicts or misleading information in the display.

- Smart monitoring in itself is of limited value. Data analysis and processing is a necessary and demanding scientific task. Decision support tools need to be integrated in energy management platforms to ensure engineers and facility managers are assisted in the accurate translation of data.

- Power predictions using ANN need to be mainstreamed and integrated in district energy management systems to provide real time control capabilities and complement demand response strategies and DR programs.

- ANN power predictions can be effectively utilised to control excess power of a microgrid and define whether energy should be stored or fed to the distribution grid.

- ANN can provide a way to determine the baseline of a customer's consumption so that changes in the power demand profile as a correspondence to a demand response event are rewarded on a commonly accepted ground.

- The implementation of cost saving measures and investments in the appropriate mix of technology can result in a low payback period and financial sustainability, a prerequisite for carrying out renovations and improving district overall efficiency.

- Apart from raising awareness campaigns or numerical displays of information difficult to interpret or relate to a users' daily routine users engagement is an emerging field with a significant gap to be exploited.

- New tools have emerged to allow users interpret dynamic pricing in a friendly and seamless way so that they can inform their energy related decisions accordingly.

- Technological advances and energy management state of the art need to be linked with sociology and management in order to address how influencing one's every day actions can be achieved in a manner not interfering with social or other values linked to the person's well-being and morals.

- Specific equipment has recently become commercially available for industrial customers and other district level demand response applications to be implemented in wide scale.

- Smart metering can be effectively implemented to assist in the appropriate planning of Advanced Metering Infrastructure, increase penetration of renewable energy and in the identification of power quality deviations. Essentially, this increases the power grid capabilities and decreases the risks associated with voltage flickering which can trigger health problems.

- Smart metering can also produce social benefits as there will be a reduction of energy loss in the power grid but also as this is one of the technical

upgrades for linking the cost of energy consumption to the costs of production, transfer and distribution of energy.

645677 — SMART GEMS — H2020-MSCA-RISE-2014
D4.3 Lessons learnt from the existing smart / micro grids. Guidelines for scaling-up the existing
infrastructure using mobile connectivity

5. Conclusions

In this report several activities performed during the staff exchange of industrial and academic partners in the Smart GEMS consortium were presented. Work included research related to the operational analysis of smart microgrids and the development of smart metering applications. Various issues have been raised and a set of guidelines have been drawn to inform the procedures for scaling up of existing smart / micro grid infrastructure. Smart monitoring and data exploitation for energy planning and demand response was explored. Power consumption and production predictions based on Artificial Neural Network models were tested and proven to be a robust technique for the implementation of Demand Response control strategies and evaluation of savings. On the utility side, it was demonstrated that smart metering can contribute to the advancement of smart grids not just by measuring and transmitting data of energy flows, or by executing remote control but also via dynamically establishing sources of voltage flickering and dealing with power quality issues. Finally, communication protocols and encryption methods were tested as part of the required advancements for the new generation smart meters. Overall experience shows that smart grid developments are an ongoing progress and step by step continuous and systematic efforts are vital for the transition of the technical, regulatory and market aspects.

6. References

[1] I. Colak, S. Sagiroglu, G. Fulli, M. Yesilbudak, and C.-F. Covrig, "A survey on the critical issues in smart grid technologies," *Renew. Sustain. Energy Rev.*, vol. 54, pp. 396–405, 2016.

[2] L. Meng, E. R. Sanseverino, A. Luna, T. Dragicevic, J. T. Vasquez, and J. . Guerrero, "Microgrid supervisory controllers and energy management systems: A literature review," *Renew. Sustain. Energy Rev.*, vol. 60, pp. 1263–1273, 2016.

[3] X. Pan, X. Niu, X. Yang, B. Jacquet, and D. Zheng, "Microgrid energy management optimization using model predictive control: a case study in China," *IFAC-PapersOnLine*, vol. 48, no. 30, pp. 306–311, 2015.

[4] A. Mahmood, N. Javaid, and S. Razzaq, "A review of wireless communications for smart grid," *Renew. Sustain. Energy Rev.*, vol. 41, pp. 248–260, 2015.

[5] D. Kolokotsa *et al.*, "Development of a web based energy management system for University Campuses: The CAMP-IT platform," *Energy Build.*, vol. 123, pp. 119–135, 2016.

[6] A. R. Khan, A. Mahmood, A. Safdar, Z. A. Khan, and N. A. Khan, "Load forecasting, dynamic pricing and DSM in smart grid: A review," *Renew. Sustain. Energy Rev.*, vol. 54, pp. 1311–1322, 2016.

[7] S. Gaurav, C. Birla, A. Lamba, S. Umashankar, and S. Ganesan, "Energy Management of PV – Battery Based Microgrid System," *Procedia Technol.*, vol. 21, pp. 103–111, 2015.

[8] S. Wenbo, L. Eun-Kyu, Y. Daoyuan, H. Rui, C. Chi-Cheng, and G. Rajit, "Evaluating microgrid management and control with an implementable energy management system," in *IEEE Smart Grid Communications (SmartGridComm)*, 2014.

[9] M. Q. Raza and A. Khosravi, "A review on artificial intelligence based load demand forecasting techniques for smart grid and buildings," *Renew. Sustain. Energy Rev.*, vol. 50, pp. 1352–1372, 2015.

[10] E. Provata, D. Kolokotsa, S. Papantoniou, M. Pietrini, A. Giovannelli, and G. Romiti, "Development of optimization algorithms for the Leaf Community microgrid," *Renew. Energy*, vol. 74, pp. 782–795, Feb. 2015.

[11] S. Sepasi, E. Reihani, A. M. Howlader, L. R. Roose, and M. M. Matsuura, "Very short term load forecasting of a distribution system with high PV penetration," *Renew. Energy*, vol. 106, pp. 142–148, 2017.

[12] M. Beccali, M. Cellura, V. Lo Brano, and A. Marvuglia, "Forecasting daily urban electric load profiles using artificial neural networks," *Energy Convers. Manag.*, vol. 45, no. 18–19, pp. 2879–2900, 2004.

[13] M. Q. Raza, M. Nadarajah, D. Q. Hung, and Z. Baharudin, "An intelligent hybrid short-term load forecasting model for smart power grids," *Sustain. Cities Soc.*, vol. 31, pp. 264–275, 2017.

[14] "MATLAB - MathWorks." [Online]. Available: https://www.mathworks.com/products/matlab.html. [Accessed: 05-Apr-2017].

[15] A. Mellit and A. M. Pavan, "A 24-h forecast of solar irradiance using artificial neural network: Application for performance prediction of a grid-connected PV plant at Trieste, Italy," *Sol. Energy*, vol. 84, no. 5, pp. 807–821, 2010.

[16] N. Kampelis, "Εφαρμογή Τεχνικών Ενεργειακού Σχεδιασμού στο Πολυτεχνείο Κρήτης [Implementation of Energy Design Techniques at the Technical University of Crete]," 2014.

[17] P. Tino, L. Benuskova, and A. Sperduti, "Artificial Neural Network Models," vol. 8, no. 3, pp. 455–472, 1997.

[18] C. T. Yang, R. Marsooli, and M. T. Aalami, "Evaluation of total load sediment transport formulas using ANN," *Int. J. Sediment Res.*, vol. 24, no. 3, pp. 274–286, 2009.

[19] C. Stergiou and D. Siganos, "Neural Networks." [Online]. Available: https://www.doc.ic.ac.uk/~nd/surprise_96/journal/vol4/cs11/report.html. [Accessed: 23-Sep-2017].

[20] A. Cerskus *et al.*, "Smart Grid Energy Management Staff Exchange: D3 . 3 Zero energy buildings and integration with smart grids : Components , Services , Systems & Controls," 2014.

[21] J. P. S. Catalao, S. J. P. S. Mariano, V. F. . Mendes, and L. A. F. . Ferreira, "Short-term electricity prices forecasting in a competitive market: A neural network approach," *Electr. Power Syst. Res.*, vol. 77, no. 10, pp. 1297–1304, 2007.

[22] A. Mavrigiannaki, N. Kampelis, D. Kolokotsa, and D. Marchegianni, "24h Forecasting of Micro-grid Excess Production," vol. 0, no. July, pp. 5–7, 2017.

[23] K. Voss *et al.*, "Load Matching and Grid Interaction of Net Zero Energy Building," *Proc. Build. Simul. 2011*, vol. 6, pp. 14–16, 2011.

[24] British Standards, "BSI Standards Publication Electromagnetic Compatibility (EMC) Part 4-12: Testing and measurement techniques - Ring wave immunity test," vol. 3, no. 1, 2011.

[25] IEEE, *IEEE 1453 - IEEE Recommended Practice for the Analysis of Fluctuating Installations on Power Systems*, vol. 2015. 2015.

[26] G. P. Colnago, J. R. Macedo, and J. L. de Freitas Vieira, "Implementation of a light Flickermeter in a low cost embedded system," *IET Sci. Meas. Technol.*, Mar. 2015.

[27] J. J. Gutierrez, I. Azcarate, P. Saiz, A. Lazkano, L. A. Leturiondo, and K. Redondo, "An alternative strategy to improve the flicker severity measurement," *Int. J. Electr. Power Energy Syst.*, vol. 63, pp. 667–673, 2014.

[28] I. Azcarate, J. J. Gutierrez, P. Saiz, A. Lazkano, L. A. Leturiondo, and K. Redondo, "Flicker characteristics of efficient lighting assessed by the IEC flickermeter," *Electr. Power Syst. Res.*, vol. 107, pp. 21–27, 2014.

[29] P. S. Wright and P. Clarkson, "Sensitivity analysis of flickermeter implementations to waveforms for testing to the requirements of IEC 61000-4-15," *IET Sci. Meas. Technol.*, vol. 4, no. 3, pp. 125–135, May 2010.

[30] J. Ruiz, J. J. Gutierrez, A. Lazkano, and S. Ruiz De Gauna, "A review of flicker severity assessment by the IEC flickermeter," *IEEE Trans.*

645677 — SMART GEMS — H2020-MSCA-RISE-2014
D4.3 Lessons learnt from the existing smart / micro grids. Guidelines for scaling-up the existing
infrastructure using mobile connectivity

Instrum. Meas., vol. 59, no. 8, pp. 2037–2047, 2010.

[31] W. Mombauer, "Calculating a new reference point for the iec-flickermeter," *Eur. Trans. Electr. Power*, vol. 8, pp. 429–436, 1998.

[32] E. Lai, *Practical Digital Signal Processing For Engineers and Technicians*. 2004.

[33] Http://www.npl.co.uk/, "Flickermeter Filter Design and Implementation." .

[34] W. Mombauer, "Flicker-simulation and minimization," *CIRED,10th Int. Conf. Electr. Distrib.*, vol. 53, no. 4798, p. 160, 1989.

[35] E. C. Ifeachor and B. W. Jervis, *Digital Signal Processing: A Practical Approach*. 1993.

[36] European Commission, "Benchmarking smart metering deployment in the EU-27 with a focus on electricity," 2014.

[37] "Overview / excerpts of the DLMS UA coloured book." [Online]. Available: http://www.dlms.com/documentation/overviewexcerptsofthedlmsuacolou redbooks/index.html.

[38] D. A. McGrew and J. Viega, *The Galois/Counter Mode of Operation (GCM)*. 2005.

[39] G. M. Weinberg, *Fuzz Testing and Fuzz History*. .

[40] R. Broadridge, *Power line modems and networks*. London UK, 1989.

[41] "M-Bus." [Online]. Available: http://www.m-bus.com/.

[42] "icube software." [Online]. Available: https://icube.ch/.

[43] "AES-GCM-Python." [Online]. Available: https://github.com/bozhu/AES-GCM-Python.